

NASA TECHNICAL NOTE



NASA TN D-4687

2.1

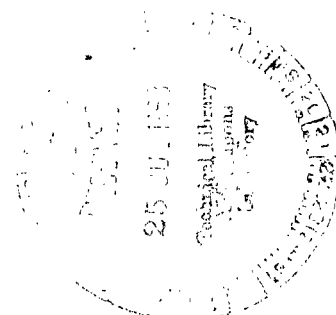


NASA TN D-4687

LOAN COPY: RETURN TO  
AFWL (WL0L-2)  
KIRTLAND AFB, N MEX

# MEMBRANE ANALYSIS OF SCALLOPED SHELLS

*by Ravindra K. Vyas*  
*Ames Research Center*  
*Moffett Field, Calif.*





0131079

NASA TN D-4687

## MEMBRANE ANALYSIS OF SCALLOPED SHELLS

By Ravindra K. Vyas

Ames Research Center  
Moffett Field, Calif.

NATIONAL AERONAUTICS AND SPACE ADMINISTRATION

---

For sale by the Clearinghouse for Federal Scientific and Technical Information  
Springfield, Virginia 22151 - CFSTI price \$3.00

# MEMBRANE ANALYSIS OF SCALLOPED SHELLS

By Ravindra K. Vyas

Ames Research Center

## SUMMARY

The main objective of this report is to contribute to the understanding of membrane forces in scalloped shells, particularly scalloped paraboloids. It is shown how the stress function approach, used successfully in the membrane analysis of elliptic and hyperbolic paraboloids, can be applied to the scalloped paraboloids. In order to demonstrate the technique, two scalloped structures having practical significance as structural models for parachutes are discussed in detail. In the cases considered, it is shown that the stress function must satisfy a linear second-order partial-differential equation with variable coefficients. The basic method for solving this equation is given in the first appendix. For comparison purposes, numerical results for similar shells of revolution are also presented. These results show that the hoop and meridional stresses in the parachute type structure are lower than those in a corresponding shell of revolution. More significantly, the meridional stress in the parachute type shell decreases remarkably, and even becomes compressive, as the bulge of the scallop, defined by a positive parameter  $\beta$ , is increased. It is shown how a critical value,  $\beta_{cr}$ , of this bulge parameter can be obtained below which the shell would remain in a compressionless state. A singular solution used in prescribing rope tension near the opening of the parachute type shell may also be useful in other aspects of parachute analysis.

A brief review of the scope and the limitations of the method and the possibility of extending it to other scalloped shells of the same family, is presented in a separate section. Suggestions for further work are included in the concluding remarks.

## INTRODUCTION

The advent of the space age is largely responsible for a growing interest in new structural concepts and techniques. Promising among the newer concepts are those of filament-wound structures and expandable structures. With these advances in technology, there exists a parallel need for theoretical investigations of different structural forms. The membrane analysis of one such form, the scalloped shell, is presented in this report.

As opposed to shells of revolution, scalloped shells have been relatively unexplored as structural forms. The parachute is, perhaps, the only form of scalloped structure that has been studied in any detail. An interesting history of the parachute and its development as a decelerating device is given in reference 1, which contains, in addition, valuable information

about various aspects of parachute performance and design. The earliest published attempts at parachute stress analysis date from 1923 when the work of Taylor, Southwell, Griffiths, Jones, and Williams, on ideal shapes of parachutes, was compiled by R. Jones in reference 2. Since then, several authors have continued this work, studying the many different aspects of parachute performance and design.

Most of the work concerning parachutes has been based on certain simplifying assumptions regarding the character of stresses in the surface. These assumptions can be broadly classified into three categories as follows:

(a) The circumferential stress in the parachute is either negligible (ref. 2) or negligible within a certain critical radius (ref. 3). This position was taken by the early investigators; (b) It is the meridional stress which is negligible rather than the hoop stress (refs. 4 and 5); (c) The circumferential stress is proportional to the product of the applied pressure and a reference radius. The meridional stress is assumed either negligible, for certain cases, or obtainable from the conditions of equilibrium (ref. 6).

The present work differs from parachute stress analysis in two important respects. First, the emphasis here is on the membrane analysis of scalloped surfaces as shell structures. The shells discussed in detail belong to the general class of surfaces designated as bulged or scalloped paraboloids, of which the parachute type structure is only one member. Secondly, since the investigation is based on the membrane theory of shells, no a priori assumptions are necessary regarding the nature of stresses - and none are made.

The method of analysis relies on the stress function approach postulated in the membrane theory of shells of arbitrary shape. This stress function approach has been successfully used in the past for solving the problems of elliptic and hyperbolic paraboloids, and it is shown in this report that this method can also be successfully applied to a more general class of scalloped shells, which includes the scalloped paraboloids as special cases. In order to demonstrate the method, the solutions for two different types of scalloped structures are discussed in detail. Since the loading and boundary conditions prescribed for these two structures could also apply to comparable parachutes, it is conceivable that these structures could serve as structural models for parachutes.

The technique used in this paper can also be applied to a wider variety of loading and edge conditions than those considered in the two examples. A more detailed discussion of the scope and the limitations of the method is given in a separate section.

#### NOTATION

A surface parameter used to define the scalloped paraboloids  
 $A_m$  undetermined coefficients associated with the homogeneous solutions  $\Psi_{Hm}$   
a reference radius, also maximum radius

$a_{m,n}$	coefficients of a power series in $x$ (appendix B)
$B_m$	undetermined coefficients associated with the homogeneous solutions $\Psi_{Hm}$
$b$	radial distance to the inner opening
$C_{m,n}, D_{m,n}$	coefficients of power series in $x$ (appendix A)
$F(\rho, x)$	function of $\rho$ and $x$ ; denotes right hand side of an inhomogeneous partial differential equation
$\left. \begin{matrix} F_m(x), F_\alpha(x) \\ F_\beta(x), F_\gamma(x) \end{matrix} \right\}$	functions of $x$
$f_m(x)$	function of $x$
$f_n$	normal component of the forces acting on the rope (fig. 9)
$f_\alpha(x), f_\beta(x)$	functions of $x$
$\left. \begin{matrix} g_m(x), g_\alpha(x) \\ g_\beta(x) \end{matrix} \right\}$	functions of $x$
$h$	normal distance from the apex of the shell to a horizontal plane passing through the point ( $r = a, \theta = 0$ )
$k$	constant associated with a singular solution; also a subscript
$k_{cr}$	critical value of the constant $k$
$L$	linear differential operator
$m$	summation index; also subscript
$N$	number of segments or gores
$N_r, N_\theta, N_{r\theta}$	membrane forces per unit length in the tangential plane of the shell (fig. 2)
$\bar{N}_r, \bar{N}_\theta, \bar{N}_{r\theta}$	projected membrane forces (fig. 2)
$n$	summation index; also denotes a power of $r$ and powers of $x$
$n_r, n_\theta, n_{r\theta}$	dimensionless membrane forces
$P$	concentrated load at the apex in the $Z$ direction
$p$	reference load intensity, also uniform normal pressure
$p_r, p_\theta, p_z$	$r, \theta, z$ components of the load intensity

$\bar{p}_r, \bar{p}_\theta, \bar{p}_z$	reduced load intensities
$Q(x)$	function of $x$ (appendix B)
$q_r, q_\theta, q_z$	dimensionless load intensities
$R(x)$	function of $x$ (appendix B)
$r$	polar distance in cylindrical coordinates (fig. 1), also a subscript
$s$	summation index
$T$	rope tension
$u_m(x)$	function of $x$ (appendix A)
$x$	transformed coordinate corresponding to the angular distance $\theta$ in polar coordinates
$x_0$	constant used in defining the range of the variable $x$
$y(x)$	function of $x$ (appendix B)
$Z(r, \theta)$	vertical coordinate defined as a function of polar coordinates $r, \theta$ to define the middle surface of the shell
$\alpha$	angle between a tangent to the middle surface and the $r$ direction; also used as a subscript and to denote a power of the variable $\rho$
$\alpha_n, \alpha_n', \alpha_n''$	coefficients of powers of $x$ in the series solutions
$\beta$	bulge parameter used in defining the scalloped paraboloids; also used as a subscript
$\beta_{cr}$	critical value of the bulge parameter
$\beta_n, \beta_n', \beta_n''$	coefficients of powers of $x$ in the series solutions
$\gamma$	angle between a tangent to the middle surface and the $\theta$ direction; also used as a subscript, denotes power of $\rho$
$\gamma_n, \gamma_n'$	coefficients of powers of $x$ (appendix A)
$\delta$	denotes a power of $\rho$
$\delta_n$	coefficients of powers of $x$ (appendix B)
$\theta$	angular distance in cylindrical coordinates (fig. 1)

$\theta_0$	constant used in defining the range of the variable $\theta$
$\lambda_k$	used to denote powers of $\rho$ in the separated solution
$\lambda_m$	eigenvalues
$\mu$	constant, describes the ratio of height $h$ to the maximum radius $a$
$\mu_n$	coefficients of power series in $x$ (appendix B)
$\mu_\alpha, \mu_\beta$	constants of integration (appendix A)
$\xi$	constant related to prescribed edge forces (fig. 10(b))
$\rho$	dimensionless radial distance
$\rho_0$	dimensionless radius corresponding to an opening at $r = b$
$\Phi(r, \theta)$	postulated stress function
$\Phi_k(x)$	homogeneous solution corresponding to the separated form $\rho^{\lambda_k} \Phi_k(x)$
$\Psi(\rho, x)$	dimensionless stress function
$\Psi_H$	solution of a homogeneous differential equation subject to homogeneous boundary conditions
$\Psi_{Hm}$	homogeneous solutions corresponding to eigenvalues $\lambda_m$
$\Psi_p$	particular solution of an inhomogeneous differential equation subject to inhomogeneous boundary conditions

#### Subscripts

cr	critical values of parameters
H	homogeneous solution
Hm	individual components of homogeneous solution
p	particular solution

#### MEMBRANE EQUATIONS

Consider a thin shell whose middle surface is defined by the relationship

$$Z = Z(r, \theta)$$

which expresses the vertical coordinate  $Z$  of the middle surface as a function of the polar coordinates,  $r, \theta$  (fig. 1). A differential element of this surface is shown enlarged in figure 2. The element is contained between two adjacent vertical planes,  $\theta = \text{constant}$ , and two adjacent vertical cylinders,  $r = \text{constant}$ . It is acted upon by the loads  $p_r, p_\theta, p_z$  (per unit area of the middle surface) and supported by the membrane forces  $N_r, N_\theta, N_{r\theta}$ . The latter quantities are forces per unit length of the line element through which they are transmitted.

The membrane equations, which  $N_r, N_\theta, N_{r\theta}$  must satisfy in order to assure equilibrium, can be conveniently written in terms of the projected<sup>1</sup> stress resultants  $\bar{N}_r, \bar{N}_\theta, \bar{N}_{r\theta}$  and the reduced load intensities  $\bar{p}_r, \bar{p}_\theta, \bar{p}_z$  as follows:

$$\frac{1}{r} \frac{\partial}{\partial r} (r \bar{N}_r) + \frac{1}{r} \frac{\partial}{\partial \theta} (\bar{N}_{r\theta}) - \frac{\bar{N}_\theta}{r} = -\bar{p}_r \quad (1a)$$

$$\frac{1}{r} \frac{\partial}{\partial \theta} (\bar{N}_\theta) + \frac{\partial}{\partial r} (\bar{N}_{r\theta}) + 2 \frac{\bar{N}_{r\theta}}{r} = -\bar{p}_\theta \quad (1b)$$

$$\frac{1}{r} \frac{\partial}{\partial r} \left( r \frac{\partial Z}{\partial r} \bar{N}_r \right) + \frac{1}{r} \frac{\partial}{\partial r} \left( \frac{\partial Z}{\partial \theta} \bar{N}_{r\theta} \right) + \frac{1}{r} \frac{\partial}{\partial \theta} \left( \frac{\partial Z}{\partial r} \bar{N}_{r\theta} \right) + \frac{1}{r} \frac{\partial}{\partial \theta} \left( \frac{1}{r} \frac{\partial Z}{\partial \theta} \bar{N}_\theta \right) = -\bar{p}_z \quad (1c)$$

where

$$\left. \begin{aligned} \bar{N}_r &= \frac{\cos \alpha}{\cos \gamma} N_r \\ \bar{N}_\theta &= \frac{\cos \gamma}{\cos \alpha} N_\theta \\ \bar{N}_{r\theta} &= N_{r\theta} \end{aligned} \right\} \quad (2)$$

$$\left. \begin{aligned} \bar{p}_r &= \frac{(\cos^2 \gamma + \cos^2 \alpha \sin^2 \gamma)^{1/2}}{\cos \alpha \cos \gamma} p_r \\ \bar{p}_\theta &= \frac{(\cos^2 \gamma + \cos^2 \alpha \sin^2 \gamma)^{1/2}}{\cos \alpha \cos \gamma} p_\theta \\ \bar{p}_z &= \frac{(\cos^2 \alpha + \cos^2 \alpha \sin^2 \gamma)^{1/2}}{\cos \alpha \cos \gamma} p_z \\ \tan \alpha &= \frac{\partial Z}{\partial r} \\ \tan \gamma &= \frac{1}{r} \frac{\partial Z}{\partial \theta} \end{aligned} \right\} \quad (3)$$

---

<sup>1</sup>Projected on a plane  $z = \text{const.}$  (fig. 2).



With the introduction of the following dimensionless stress resultants and load intensities,

$$\left. \begin{aligned} n_r &= \frac{\bar{N}_r}{pa} \\ n_\theta &= \frac{\bar{N}_\theta}{pa} \\ n_{r\theta} &= \frac{\bar{N}_{r\theta}}{pa} \end{aligned} \right\} \quad (4)$$

$$\left. \begin{aligned} q_r &= \frac{\bar{p}_r}{p} \\ q_\theta &= \frac{\bar{p}_\theta}{p} \\ q_z &= \frac{\bar{p}_z}{p} \end{aligned} \right\} \quad (5)$$

where  $p$  is a reference load intensity and  $a$  is a reference radius  $\geq r$ , the equations (1a) - (1c) can be written as follows:

$$\frac{\partial}{\partial r} (n_r) + \frac{1}{r} \frac{\partial}{\partial \theta} (n_{r\theta}) + \frac{n_r - n_\theta}{r} = - \frac{q_r}{a} \quad (6a)$$

$$\frac{1}{r} \frac{\partial}{\partial \theta} (n_\theta) + \frac{\partial}{\partial r} (n_{r\theta}) + 2 \frac{n_{r\theta}}{r} = - \frac{q_\theta}{a} \quad (6b)$$

$$\begin{aligned} \left( \frac{\partial^2 Z}{\partial r^2} + \frac{1}{r} \frac{\partial Z}{\partial r} \right) n_r + \frac{2}{r} \frac{\partial^2 Z}{\partial r \partial \theta} n_{r\theta} + \frac{1}{r^2} \frac{\partial^2 Z}{\partial \theta^2} n_\theta + \frac{\partial Z}{\partial r} \frac{\partial n_r}{\partial r} + \frac{1}{r} \frac{\partial Z}{\partial \theta} \frac{\partial n_{r\theta}}{\partial r} \\ + \frac{1}{r} \frac{\partial Z}{\partial r} \frac{\partial n_{r\theta}}{\partial \theta} + \frac{1}{r^2} \frac{\partial Z}{\partial \theta} \frac{\partial n_\theta}{\partial \theta} = - \frac{q_z}{a} \end{aligned} \quad (6c)$$

Equations (6a) - (6c) are applicable to any shell surface of arbitrary shape, in cylindrical coordinates, so long as there exists a one-to-one correspondence between points of the middle surface of the shell and their projections on a horizontal plane ( $Z = \text{const.}$ ). If the forces  $n_r, n_\theta, n_{r\theta}$  are defined in terms of an Airy type stress function  $\Phi(r, \theta)$  such that

$$\left. \begin{aligned} n_r &= \frac{1}{r} \frac{\partial \Phi}{\partial r} + \frac{1}{r^2} \frac{\partial^2 \Phi}{\partial \theta^2} - \frac{1}{r} \int r \frac{q_r}{a} dr - \frac{1}{r} \int r \int \frac{q_\theta}{a} d\theta dr \\ n_\theta &= \frac{\partial^2 \Phi}{\partial r^2} - r \int \frac{q_\theta}{a} d\theta \\ n_{r\theta} &= \frac{1}{r^2} \frac{\partial \Phi}{\partial \theta} - \frac{1}{r} \frac{\partial^2 \Phi}{\partial r \partial \theta} \end{aligned} \right\} \quad (7)$$

then, it can be verified that equations (6a) and (6b) are automatically satisfied and equation (6c) reduces to:

$$\begin{aligned} &\left( \frac{1}{r} \frac{\partial Z}{\partial r} + \frac{1}{r^2} \frac{\partial^2 Z}{\partial \theta^2} \right) \frac{\partial^2 \Phi}{\partial r^2} + \left( \frac{2}{r^3} \frac{\partial Z}{\partial \theta} - \frac{2}{r^2} \frac{\partial^2 Z}{\partial r \partial \theta} \right) \frac{\partial^2 \Phi}{\partial r \partial \theta} \\ &+ \left( \frac{1}{r^2} \frac{\partial^2 Z}{\partial r^2} \right) \frac{\partial^2 \Phi}{\partial \theta^2} + \left( \frac{1}{r} \frac{\partial^2 Z}{\partial r^2} \right) \frac{\partial \Phi}{\partial r} + \left( \frac{2}{r^3} \frac{\partial^2 Z}{\partial r \partial \theta} - \frac{2}{r^4} \frac{\partial Z}{\partial \theta} \right) \frac{\partial \Phi}{\partial \theta} \\ &= - \frac{q_z}{a} + \frac{\partial Z}{\partial r} \frac{q_r}{a} + \frac{1}{r} \frac{\partial Z}{\partial \theta} \frac{q_\theta}{a} + \left( \frac{1}{r} \frac{\partial^2 Z}{\partial \theta^2} + \frac{\partial Z}{\partial r} \right) \int \frac{q_\theta}{a} d\theta \\ &+ \frac{\partial^2 Z}{\partial r^2} \left( \frac{1}{r} \int r \frac{q_r}{a} dr + \frac{1}{r} \int r dr \int \frac{q_\theta}{a} d\theta \right) \quad (8)^2 \end{aligned}$$

The governing equation (8) is a second-order partial differential equation, and, depending on the choice of surface, may have either constant or variable coefficients. The stress function approach has been successfully used in the past for solving problems of elliptic and hyperbolic paraboloids. For each of these cases equation (8) has constant coefficients and is reducible to a standard form: the former to the Poisson's equation, the latter to the wave equation. In the case of the scalloped paraboloids, equation (8) has variable coefficients, as will be seen later.

### THE SCALLOPED PARABOLOID

The middle surface of the scalloped or bulged paraboloids may be defined by the relationship

$$Z = Ar^2(1 + \beta\theta^2) , \quad -\theta_0 \leq \theta \leq \theta_0 , \quad \theta_0 \leq \pi , \quad \beta > 0 \quad (9)^3$$

---

<sup>2</sup>Reference 7 gives a similar formulation in rectangular coordinates.

<sup>3</sup>The shell surface, it may be noted, is symmetric with respect to the plane  $\theta = 0$ .

where  $A, \beta$  are constants. The parameter  $\beta$  defines the bulge of the scalloped surface and may be called the bulge parameter. It should be noted that when  $\beta$  equals zero, equation (9) describes a paraboloid of revolution, hence, the designation "bulged" or "scalloped" paraboloid.

Such a shell, like any other structure, can be loaded in many different ways. As a roof structure, it may be loaded by gravitational and wind loads. As a pressure vessel bulkhead, it may be subjected to a uniform or varying normal pressure. As a parachute type structure, a uniform normal pressure would constitute a reasonable loading. In the analysis to follow, a uniform normal pressure will be assumed.

Assuming the surface segment defined by equation (9), then the load intensities, the definitions (3) and (4), and the equilibrium condition (8) take the form

$$\left. \begin{aligned}
 p_r &= \frac{\sin \alpha \cos \gamma}{(\cos^2 \alpha + \cos^2 \alpha \sin^2 \gamma)^{1/2}} p \\
 p_\theta &= \frac{\cos \alpha \sin \gamma}{(\cos^2 \alpha + \cos^2 \alpha \sin^2 \gamma)^{1/2}} p \\
 p_z &= - \frac{\cos \alpha \cos \gamma}{(\cos^2 \alpha + \cos^2 \alpha \sin^2 \gamma)^{1/2}} p \\
 \bar{p}_r &= \tan \alpha p \\
 \bar{p}_\theta &= \tan \gamma p \\
 \bar{p}_z &= -p \\
 q_r &= \tan \alpha \\
 q_\theta &= \tan \gamma \\
 q_z &= -1
 \end{aligned} \right\} \quad (10)$$

where

$$\tan \alpha = 2Ar(1 + \beta\theta^2)$$

$$\tan \gamma = 2Ar\beta\theta$$

and

$$\begin{aligned}
& (1 + \beta + \beta\theta^2) \frac{\partial^2 \Phi}{\partial r^2} + (1 + \beta\theta^2) \frac{1}{r^2} \frac{\partial^2 \Phi}{\partial \theta^2} - 2\beta\theta \cdot \frac{1}{r} \frac{\partial^2 \Phi}{\partial r \partial \theta} \\
& + (1 + \beta\theta^2) \frac{1}{r} \frac{\partial \Phi}{\partial r} + 2\beta\theta \cdot \frac{1}{r^2} \frac{\partial \Phi}{\partial \theta} \\
& = \frac{1}{2Aa} + \frac{Ar^2}{a} \left[ \frac{8}{3} + \left( \frac{20}{3} + 3\beta \right) \beta\theta^2 + 4\beta^2\theta^4 \right] \quad (11)
\end{aligned}$$

Next, introduce the transformation

$$\left. \begin{aligned} \rho &= r/a \\ x &= \sqrt{\beta} \theta \end{aligned} \right\} \quad (12)$$

where  $a$  is a reference radius, and define

$$\Phi(r, \theta) = a^2 \Psi(\rho, x) \quad (13)$$

$$\left. \begin{aligned} h &= \mu a \\ \mu &= \text{constant} \end{aligned} \right\} \quad (14)$$

The coordinate  $\rho$  in equations (12) is a dimensionless radius; the coordinate  $x$ , which is linearly related to  $\theta$ , is introduced for convenience in algebraic and numerical work, and the stress function  $\Psi$  in equation (13) is a dimensionless function. The height  $h$ , designated as the normal distance from the apex to a horizontal plane passing through the point  $r = a$ ,  $\theta = 0$ , is defined in equations (14) as a certain multiple of the reference radius  $a$ . If equations (12) - (14) are substituted into equation (11), it can be shown that the stress function  $\Psi(\rho, x)$  must satisfy the differential equation:

$$L(\Psi) = F(\rho, x) \quad (15)$$

where  $L$  is the linear differential operator defined by

$$\begin{aligned}
L = & \left[ (1 + \beta + x^2) \frac{\partial^2}{\partial \rho^2} + (1 + x^2) \frac{1}{\rho} \frac{\partial}{\partial \rho} \right. \\
& \left. + (1 + x^2) \frac{\beta}{\rho^2} \frac{\partial^2}{\partial x^2} - 2\beta x \frac{1}{\rho} \frac{\partial^2}{\partial \rho \partial x} + 2\beta x \frac{1}{\rho^2} \frac{\partial}{\partial x} \right] \quad (16)
\end{aligned}$$

and

$$F(\rho, x) = \frac{1}{2\mu} + \mu\rho^2 \left[ \frac{8}{3} + \left( 3\beta + \frac{20}{3} \right) x^2 + 4x^4 \right] \quad (17)$$

In terms of the dimensionless stress function  $\Psi$  and the variables  $\rho, x$  the membrane forces  $n_r, n_\theta, n_{r\theta}$  can now be expressed as follows:

$$\left. \begin{aligned} n_r &= \frac{1}{\rho} \frac{\partial \Psi}{\partial \rho} + \frac{\beta}{\rho^2} \frac{\partial^2 \Psi}{\partial x^2} - \mu \rho^2 \left( \frac{2}{3} + x^2 \right) \\ n_\theta &= \frac{\partial^2 \Psi}{\partial \rho^2} - \mu \rho^2 x^2 \\ n_{r\theta} &= \sqrt{\beta} \left( \frac{1}{\rho^2} \frac{\partial \Psi}{\partial x} - \frac{1}{\rho} \frac{\partial^2 \Psi}{\partial \rho \partial x} \right) \end{aligned} \right\} \quad (18)$$

Membrane analysis of the scalloped shell, therefore, reduces to the mathematical problem of solving equation (15) subject to appropriate boundary conditions. The equation, as can be seen, is a linear second-order partial differential equation with variable coefficients, and includes all the derivatives of the stress function  $\Psi$  up to the second order. It does not seem possible to reduce it to a known standard form, though it can be solved, as will be shown in appendix A, by the method of separation of variables.

In the next two sections, solutions of equation (15) will be discussed in detail, along with numerical results, for two particular types of structures, namely the single scallop and the parachute type structure. The latter is so called because of its similarity to a parachute in surface geometry, loading and boundary conditions. In each case, the numerical results for a similar shell of revolution will also be given for comparison purposes. It will be seen that the basic mathematical approach outlined in appendix A applies equally to both cases and yields solutions that are very similar in form.

### THE SINGLE SCALLOP

Consider the symmetric scalloped shell shown in figure 3. It will be assumed for this particular example that the edge members in the vertical planes  $\theta = \pm\theta_0$  cannot resist any thrust normal to their planes, so that  $N_\theta = 0$  along these edges. Furthermore, it will be assumed that  $N_r = 0$  along the edge  $r = a$ . It must be mentioned that with the technique to be presented in this section, it is also possible to prescribe other distributions of the force  $N_r$  along this boundary.

Since the structure, as well as the loading, is symmetric about the vertical plane  $\theta = 0$ , it is sufficient to assume a solution symmetric in  $\theta$  and confine the analysis to the domain  $0 \leq r \leq a$ ,  $0 \leq \theta \leq \theta_0$ . In terms of the stress function  $\Psi$  and the variables  $\rho, x$ , the mathematical problem of solving equilibrium equation (15), subject to the boundary conditions  $N_\theta(r, \theta_0) = 0$ ,  $N_r(a, \theta) = 0$ , can be described as follows:

$$L(\Psi) = F(\rho, x) \quad 0 \leq \rho \leq 1; \quad 0 \leq x \leq x_0 \quad (19a)$$

$$\frac{\partial^2 \Psi}{\partial \rho^2} = \mu \rho^2 x^2 \quad \text{at } x = x_0 \quad (19b)$$

$$\left[ \frac{1}{\rho} \frac{\partial \Psi}{\partial \rho} + \frac{\beta}{\rho^2} \frac{\partial^2 \Psi}{\partial x^2} - \mu \rho^2 \left( \frac{2}{3} + x^2 \right) \right] = 0 \quad \text{at } \rho = 1 \quad (19c)$$

The variables in equation (19a) can be separated by assuming solutions of the form  $\rho^{\lambda_k} \phi_k(x)$ , where the functions  $\phi_k(x)$  satisfy a linear ordinary second-order differential equation with variable coefficients and can be obtained in the form of an infinite series in even powers of  $x$ . By use of this approach,<sup>4</sup> the solution  $\Psi(\rho, x)$  can be obtained in the form:

$$\Psi(\rho, x) = \Psi_p(\rho, x) + \Psi_H(\rho, x) \quad (20)$$

The function  $\Psi_p$  in (20) satisfies both the inhomogeneous differential equation (19a) and the inhomogeneous boundary condition (19b), and has the form

$$\Psi_p(\rho, x) = \frac{1}{2\mu} \rho^2 \sum_{n=0,2,4,\dots} \alpha_n x^n + \mu \rho^4 \sum_{n=0,2,4,\dots} \beta_n x^n \quad (21)$$

The homogeneous solution  $\Psi_H(\rho, x)$  has the form

$$\Psi_H(\rho, x) = \sum_{m=1,2,3,\dots} A_m \Psi_{Hm}(\rho, x) \quad (22)$$

where each function  $\Psi_{Hm}$ , defined by

$$\Psi_{Hm} = \rho^{\lambda_m} F_m(x) \quad (23)$$

satisfies both the homogeneous differential equation

$$L(\Psi_{Hm}) = 0 \quad (24)$$

and the homogeneous boundary condition

$$\frac{\partial^2}{\partial \rho^2} (\Psi_{Hm}) = 0 \quad (25)$$

The values  $\lambda_m$  are the eigenvalues of the system described by equations (24) and (25). These eigenvalues occur, in the present case, as pairs of positive and negative numbers of equal magnitude, so that the corresponding homogeneous solutions take on the form  $\rho^{\lambda_m} f_m(x)$ ,  $\rho^{-\lambda_m} g_m(x)$ , where

---

<sup>4</sup>For more details see appendix A.

$$\left. \begin{aligned} f_m(x) &= \sum_{n=0,2,4,\dots} C_{m,n} x^n \\ g_m(x) &= \sum_{n=0,2,4,\dots} D_{m,n} x^n \end{aligned} \right\} \quad (26)$$

The homogeneous solution can now be written as

$$\Psi_H = \sum_{m=1,2,3,\dots} A_m \rho^{\lambda_m} \sum_{n=0,2,4,\dots} C_{m,n} x^n + \sum_{m=1,2,3,\dots} B_m \rho^{-\lambda_m} \sum_{n=0,2,4,\dots} D_{m,n} x^n \quad (27)$$

Substituting equations (21) and (27) into equation (20), the solution  $\Psi$  may be written

$$\begin{aligned} \Psi(\rho, x) &= \frac{1}{2\mu} \rho^2 \sum_{n=0,2,4,\dots} \alpha_n x^n + \mu \rho^4 \sum_{n=0,2,4,\dots} \beta_n x^n \\ &+ \sum_{m=1,2,3,\dots} A_m \rho^{\lambda_m} \sum_{n=0,2,4,\dots} C_{m,n} x^n \\ &+ \sum_{m=1,2,3,\dots} B_m \rho^{-\lambda_m} \sum_{n=0,2,4,\dots} D_{m,n} x^n \end{aligned} \quad (28)$$

Applying (28) and definitions (18), the stress resultants can be expressed as follows:

$$\begin{aligned} n_r &= \frac{1}{2\mu} \sum_{n=0,2,4,\dots} [2\alpha_n + \beta(n+2)(n+1)\alpha_{n+2}] x^n \\ &+ \mu \rho^2 \sum_{n=0,2,4,\dots} [4\beta_n + \beta(n+2)(n+1)\beta_{n+2}] x^n - \mu \rho^2 \left( \frac{2}{3} + x^2 \right) \\ &+ \sum_{m=1,2,3,\dots} A_m \rho^{\lambda_m-2} \sum_{n=0,2,4,\dots} [\lambda_m C_{m,n} + \beta(n+2)(n+1)C_{m,n+2}] x^n \\ &+ \sum_{m=1,2,3,\dots} B_m \rho^{-(\lambda_m+2)} \sum_{n=0,2,4,\dots} [-\lambda_m D_{m,n} + \beta(n+2)(n+1)D_{m,n+2}] x^n \end{aligned} \quad (29)$$

$$\begin{aligned}
n_\theta = & \frac{1}{2\mu} \sum_{n=0,2,4,\dots} 2\alpha_n x^n + \mu\rho^2 \left( \sum_{n=0,2,4,\dots} 12\beta_n x^n - x^2 \right) \\
& + \sum_{m=1,2,3,\dots} A_m \rho^{\lambda_m-2} \sum_{n=0,2,4,\dots} \lambda_m(\lambda_m - 1) C_{m,n} x^n \\
& + \sum_{m=1,2,3,\dots} B_m \rho^{-(\lambda_m+2)} \sum_{n=0,2,4,\dots} \lambda_m(\lambda_m + 1) D_{m,n} x^n \quad (30)
\end{aligned}$$

$$\begin{aligned}
n_{r\theta} = \sqrt{\beta} \left[ \frac{1}{2\mu} \sum_{n=0,2,4,\dots} -n\alpha_n x^{n-1} + \mu\rho^2 \sum_{n=0,2,4,\dots} -3n\beta_n x^{n-1} \right. \\
+ \sum_{m=1,2,3,\dots} A_m \rho^{\lambda_m-2} \sum_{n=0,2,4,\dots} n(1 - \lambda_m) C_{m,n} x^{n-1} \\
\left. + \sum_{m=1,2,3,\dots} B_m \rho^{-(\lambda_m+2)} \sum_{n=0,2,4,\dots} n(1 + \lambda_m) D_{m,n} x^{n-1} \right] \quad (31)
\end{aligned}$$

It should be observed that the homogeneous solutions associated with the negative eigenvalues are singular at the point  $\rho = 0$ , which is an included point of the domain. Consequently, the undetermined coefficients  $B_m$  associated with these solutions must be chosen as zero. The coefficients  $A_m$  can be chosen appropriately to prescribe suitable edge forces at  $\rho = 1$  (corresponding to  $r = a$ ). In particular it is possible to choose these coefficients so as to satisfy the condition prescribed in (19c). For paraboloids of revolution ( $\beta = 0$ )<sup>5</sup> the eigenfunctions  $f_m(x)$  form a set of orthogonal trigonometric functions, and the coefficients  $A_m$  can be conveniently determined by means of this orthogonality property. In the present case ( $\beta \neq 0$ ), no such orthogonality property is readily available, and it is necessary to resort to suitable numerical methods such as collocation, matching coefficients of power series, or mean square approximation. The last technique has been found to give the most satisfactory results, and its application to the case of scalloped paraboloids is described briefly in appendix B.

---

<sup>5</sup>Transformation (11) for this case is  $\theta = x$ .



Consider, as a particular example, the case  $\beta = 1$ ,  $\mu = 0.5$ ,  $\theta_0 = \pi/6$ . The homogeneous solution (22) was found to be sufficiently approximated by the six-term truncated series

$$\Psi_H = \sum_{m=1,2,\dots}^6 A_m \Psi_{Hm} = \sum_{m=1,2,\dots}^6 A_m \rho^{\lambda_m} \sum_{n=0,2,4,\dots} C_{m,n} x^n \quad (32)$$

where the eigenvalues  $\lambda_m$  and the coefficients  $A_m$  are listed in table I. These values have been obtained according to the methods discussed in the appendixes A and B. The coefficients  $\alpha_n$ ,  $\beta_n$  associated with the particular solution (21) and the coefficients  $C_{m,n}$  associated with the homogeneous solutions  $\Psi_{Hm}$  may then be evaluated by means of the recursion relationships given in appendix A. In this example, the first 25 terms of each of the series expansions in  $x$  in equations (29) - (31) were used to obtain the stress resultants presented in figures 4-7.

TABLE I.- SINGLE SCALLOP: EIGENVALUES  $|\lambda_m|$  AND THE UNDETERMINED COEFFICIENTS  $A_m$

m	$ \lambda_m $	$A_m$
1	2.26514	0.453853
2	6.63706	$-.913284 \times 10^{-2}$
3	11.0383	$.689597 \times 10^{-3}$
4	15.4446	$-.121309 \times 10^{-3}$
5	19.8525	$.134767 \times 10^{-4}$
6	24.2612	$-.286088 \times 10^{-4}$

The broken line in figure 4 represents the meridional force  $n_r$  at the edge  $\rho = 1$  due to the particular solution  $\Psi_p$ ; the solid line represents the force  $n_r$  due to this particular solution plus the homogeneous solution  $\Psi_H$  (eq. (32)). This homogeneous solution is added to obtain the desired vanishing edge force  $n_r$  along the edge  $\rho = 1$ . The difference between the broken and solid lines in figure 4 indicates the efficiency of this edge correction by the six-term approximation (32). This efficiency would improve as more solutions  $\Psi_{Hm}$  were included in (32). The forces  $n_\theta$ ,  $n_{r\theta}$  along this edge are plotted in figure 5.

For the interior points of the domain, it can be shown that only the first few homogeneous solutions are of importance, since the solutions corresponding to higher eigenvalues rapidly diminish as  $\rho$  decreases from  $\rho = 1$ . The solid lines in figures 6 and 7 represent the stress resultants in the scallop, while the broken lines represent the stress resultants in the corresponding shell of revolution ( $\beta = 0$ ). The forces  $n_r$ ,  $n_\theta$  along the central meridian (fig. 6) are lower in most parts of the scalloped shell than in the shell of revolution. The same is true for shear stress along the edge  $\theta = \theta_0$ , although along this edge the meridional force  $n_r$  is higher in the scalloped shell for a considerable distance from the apex.

It should be observed that for both types of shells the stresses tend to be relatively high in the vicinity of the three corners. These stress concentrations are pronounced, in the case of the scalloped shells, near the apex, and in the case of the shells of revolution, near the lower two corners. For either type of structure the corner regions need special attention and should be designed to withstand higher stresses than the rest of the shell.

The method of analysis for a shell terminated at an inner boundary  $r = b \neq 0$  ( $\rho = \rho_0 \neq 0$ ) would be similar. In this event, however, the solutions corresponding to the negative eigenvalues would have to be included in the analysis, since these solutions are necessary for prescribing appropriate boundary values at  $r = b$ . If the lowest eigenvalue  $|\lambda_1|$  is sufficiently high, then the coefficients  $A_m, B_m$  associated with the two sets of homogeneous solutions can be determined separately, by mean square approximation at each of the two boundaries. Otherwise, it may be necessary to use an iterative scheme, similar to the one described in reference 8, in order to obtain a satisfactory solution.

It should be noted at this point that the bulge parameter  $\beta$  has been prescribed unity only for the purpose of the numerical example. The technique places no restriction on the magnitude of this parameter, although, of course, it must always be positive, since surfaces with negative  $\beta$  belong to a different family.

#### PARACHUTE TYPE STRUCTURE

The method demonstrated in the preceding section can also be applied to the parachute type structure with an opening at the top, as shown in figure 8. In this case, however, the circumferential force  $n_\theta$  need no longer be zero at  $\theta = \pm\theta_0$ . Because of structural symmetry and symmetric loading it is sufficient to solve the problem, as for the single scallop, in the domain  $b \leq r \leq a$ ,  $0 \leq \theta \leq \theta_0$ .

The boundary condition at  $\theta = \theta_0$  can be obtained as follows. If the rope is considered an individual structure, loaded by the membrane forces from the shell at the edge  $\theta = \theta_0$ , it can be shown that the rope tension  $T$ , at any coordinate  $r$ , must satisfy the equilibrium condition (see fig. 9),

$$\begin{aligned} T &= \frac{[1 + 4A^2r^2(1 + \beta\theta_0^2)^2]^{3/2}}{2A(1 + \beta\theta_0^2)} \cdot f_n \\ &= \frac{4A\rho a\beta\theta_0 r[1 + 4A^2r^2(1 + \beta\theta_0^2)^2]^{1/2}}{2A(1 + \beta\theta_0^2)} n_\theta \end{aligned} \quad (33)$$

On the other hand, considering the entire structure above a given radius  $r$ , it follows that the rope tension  $T$  and the membrane forces  $n_r, n_{r\theta}$  must also satisfy the condition of equilibrium of vertical forces:

$$T = \frac{p[1 + 4A^2r^2(1 + \beta\theta_0^2)^2]^{1/2}}{2A(1 + \beta\theta_0^2)r} \left[ \frac{\pi r^2}{N} - \frac{P}{pN} - 4aAr^2 \int_0^{\theta_0} (1 + \beta\theta^2)n_r d\theta - 4Aar^2 \int_0^{\theta_0} \beta\theta n_{r\theta} d\theta \right] \quad (34)$$

where  $P$  is an arbitrary vertical load concentrated downward at the apex, and  $N$  is the number of scallops. The load  $P$  may be assigned any value appropriate to the problem of interest. Eliminating the rope tension  $T$  between equations (33) and (34), the boundary condition at  $\theta = \theta_0$  is obtained:

$$r^2\beta\theta_0 n_\theta(r, \theta_0) + r^2 \int_0^{\theta_0} [(1 + \beta\theta^2)n_r + \beta\theta n_{r\theta}] d\theta = \frac{\pi r^2}{4ANa} - \frac{P}{4Aa\pi N} \quad (35)$$

The boundary conditions at the edges  $r = b$  and  $r = a$  depend on the nature of the structure. For a model parachute it would be reasonable, for example, to expect an almost vanishing meridional force  $n_r$  along these boundaries: such a surface would be expected to carry the applied loads by means of tensile and shear forces alone, since the material may be assumed incapable of sustaining compressive stresses. Assuming uniform normal pressure, the governing differential equation, condition (35) and the above requirements can be described as follows:

$$L(\Psi) = F(\rho, x) \quad \rho_0 \leq \rho \leq 1; \quad 0 \leq x \leq x_0 \quad (36)$$

$$\begin{aligned} \rho^2 \beta x_0 \left( \frac{\partial^2 \Psi}{\partial \rho^2} \right)_{x=x_0} + \rho^2 \int_0^{x_0} \left[ (1 + x^2) \left( \frac{1}{\rho} \frac{\partial \Psi}{\partial \rho} + \frac{\beta}{\rho^2} \frac{\partial^2 \Psi}{\partial x^2} \right) + \beta x \left( \frac{1}{\rho^2} \frac{\partial \Psi}{\partial x} - \frac{1}{\rho} \frac{\partial^2 \Psi}{\partial \rho \partial x} \right) \right] dx \\ = \frac{x_0 \rho^2}{4\mu} + \mu \rho^4 \left[ \frac{2}{3} x_0 + \left( \beta + \frac{2}{9} \right) x_0^3 + \frac{x_0^5}{5} \right] - \frac{P\sqrt{\beta}}{4pa^2\mu N} \end{aligned} \quad (37)$$

$$n_r \approx 0 \quad \text{at} \quad \rho = \rho_0 \quad (r = b) \quad (38)$$

$$n_r \approx 0 \quad \text{at} \quad \rho = 1 \quad (r = a) \quad (39)$$

$$n_r, \quad n_\theta \geq 0 \quad (40)$$

The solution of equations (36), by the method described in appendix A, can be written in the form:

$$\begin{aligned}
\Psi(\rho, x) &= \frac{1}{2\mu} \rho^2 \sum_{n=0,2,4,\dots} \alpha_n x^n - \frac{k}{2\mu} \log(\rho \sqrt{1+x^2}) \\
&\quad + \mu \rho^4 \sum_{n=0,2,4,\dots} \beta_n x^n + \sum_{m=1,2,3,\dots} A_m \rho^{\lambda_m} \sum_{n=0,2,4,\dots} C_{m,n} x^n \\
&\quad + \sum_{m=1,2,3,\dots} B_m \rho^{-\lambda_m} \sum_{n=0,2,4,\dots} D_{m,n} x^n \\
&= \Psi_p + \Psi_H
\end{aligned} \tag{41}$$

where

$$\begin{aligned}
\Psi_p &= \frac{\rho^2}{2\mu} \sum_{n=0,2,4,\dots} \alpha_n x^n + \mu \rho^4 \sum_{n=0,2,4,\dots} \beta_n x^n - \frac{k}{2\mu} \log(\rho \sqrt{1+x^2}) \\
\Psi_H &= \sum_{m=1,2,3,\dots} A_m \rho^{\lambda_m} \sum_{n=0,2,4,\dots} C_{m,n} x^n + \sum_{m=1,2,3,\dots} B_m \rho^{-\lambda_m} \sum_{n=0,2,4,\dots} D_{m,n} x^n \\
k &= \frac{P \sqrt{\beta}}{2pa^2N} \left[ \frac{1}{(1-x_0)\beta + \beta \tan^{-1} x_0 + (x_0^3/3)} \right]
\end{aligned} \tag{42}$$

A comparison of equations (41) with (28) reveals that the forms of the two solutions differ only in the term  $k/2 \log(\rho \sqrt{1+x^2})$ . By means of equations (41), the membrane forces  $n_r, n_\theta, n_{r\theta}$  and the rope tension  $T$  can be expressed as follows:

$$\begin{aligned}
n_r &= -\frac{k}{2\mu} \frac{1}{\rho^2} \left[ 1 + \frac{\beta(1-x^2)}{(1+x^2)^2} \right] + \frac{1}{2\mu} \sum_{n=0,2,4,\dots} [2\alpha_n + \beta(n+2)(n+1)\alpha_{n+2}] x^n \\
&\quad + \mu \rho^2 \left\{ \sum_{n=0,2,4,\dots} [4\beta_n + \beta(n+2)(n+1)\beta_{n+2}] x^n - \left( \frac{2}{3} + x^2 \right) \right\} \\
&\quad + \sum_{m=1,2,3,\dots} A_m \rho^{\lambda_m-2} \sum_{n=0,2,4,\dots} [\lambda_m C_{m,n} + \beta(n+2)(n+1)C_{m,n+2}] x^n \\
&\quad + \sum_{m=1,2,3,\dots} B_m \rho^{-(\lambda_m+2)} \sum_{n=0,2,4,\dots} [-\lambda_m D_{m,n} + \beta(n+2)(n+1)D_{m,n+2}] x^n
\end{aligned} \tag{43}$$

$$\begin{aligned}
n_\theta = & \frac{k}{2\mu} \frac{1}{\rho^2} + \frac{1}{2\mu} \sum_{n=0,2,4,\dots} 2\alpha_n x^n + \mu\rho^2 \left( \sum_{n=0,2,4,\dots} 12\beta_n x^n - x^2 \right) \\
& + \sum_{m=1,2,3,\dots} A_m \rho^{\lambda_m-2} \sum_{n=0,2,4,\dots} \lambda_m(\lambda_m - 1) C_{m,n} x^n \\
& + \sum_{m=1,2,3,\dots} B_m \rho^{-(\lambda_m+2)} \sum_{n=0,2,4,\dots} \lambda_m(\lambda_m + 1) D_{m,n} x^n
\end{aligned} \tag{44}$$

$$\begin{aligned}
n_{r\theta} = & \sqrt{\beta} \left[ -\frac{k}{2\mu} \frac{1}{\rho^2} \frac{x}{1+x^2} - \frac{1}{2\mu} \sum_{n=0,2,4,\dots} n\alpha_n x^{n-1} - \mu\rho^2 \sum_{n=0,2,4,\dots} 3n\beta_n x^{n-1} \right. \\
& + \sum_{m=1,2,3,\dots} A_m \rho^{\lambda_m-2} \sum_{n=0,2,4,\dots} n(1 - \lambda_m) C_{m,n} x^n \\
& \left. + \sum_{m=1,2,3,\dots} B_m \rho^{-(\lambda_m+2)} \sum_{n=0,2,4,\dots} n(1 + \lambda_m) D_{m,n} x^n \right]
\end{aligned} \tag{45}$$

$$T = 2\mu a^2 \sqrt{\beta} x_0 \rho \frac{[1 + 4\mu^2 \rho^2 (1 + x_0^2)^2]^{1/2}}{(1 + x_0^2)} n_\theta(\rho, x_0) \tag{46}$$

The boundary conditions (38) and (39) and the requirement (40) represent perhaps an ideal situation, but the tensile requirement (40) could be satisfied even if the forces  $n_r$  were tensile at the upper and lower edges.

The stresses due to the particular solution  $\Psi_p$  are of interest in view of requirement (40). In the present investigation it has been found that for a given choice of the parameters  $N$ ,  $\rho_0$  ( $\ll 1$ ) and  $\mu$  the above requirement will be satisfactorily met if  $\beta$  and  $k$  are less than certain readily determined critical values  $\beta_{cr}$  and  $k_{cr}$ . The significance of these parameters will be discussed later. It should be observed in passing that for practical parachute models  $N$  is generally large (say  $>10$ ). In the present study it has been found that values of  $|\lambda_m|$  depend largely on  $N$  and are of the order of magnitude  $mN$ . For large  $N$ , the particular solution  $\Psi_p$  then becomes the dominant solution, and the approximate solution  $\Psi \approx \Psi_p$  can be used to obtain satisfactory values for stresses in most parts of the shell. Consider, as a numerical example, a parachute model with 12 scallops ( $N = 12$ ),  $\rho_0 = 0.1$  and  $\mu = 0.4$ . For this combination of the geometric parameters, the critical values of  $\beta$ ,  $k$  have been determined to be 0.5 and 0.0017, respectively, and the corresponding solution  $\Psi_p$  meets requirements (36) - (38). It may be

recalled here that, as for the single scallop, the two sets of homogeneous solutions associated with the positive and negative eigenvalues are to be used to satisfy proper edge conditions at the lower and upper boundaries. Since condition (38) at the upper edge is already satisfactorily met, the coefficients  $B_m$ , associated with the solutions in  $\rho^{-\lambda_m}$ , may be appropriately chosen as zero. Furthermore, with  $\beta = \beta_{cr}$ , the edge forces  $n_r$  at  $\rho = 1$  due to the particular solution are already very small, and a five-term truncated series for  $\Psi_H$  satisfactorily meets requirement (39). The corresponding five values of  $\lambda_m$ ,  $A_m$  are listed in table II.

TABLE II.- PARACHUTE TYPE STRUCTURE: THE CONSTANT  $k$ ,  
THE EIGENVALUES  $|\lambda_m|$  AND THE UNDETERMINED  
COEFFICIENTS  $A_m$

$$k = 0.001726$$

m	$ \lambda_m $	$A_m$
1	12.7379	$-0.248942 \times 10^{-3}$
2	23.3730	$.200055 \times 10^{-4}$
3	33.5535	$-.488396 \times 10^{-5}$
4	43.5804	$.179266 \times 10^{-5}$
5	53.5374	$-.115634 \times 10^{-5}$

Before discussing the results for this case and a similar shell of revolution, it is necessary to contrast certain features of the solutions for the two types of structures. For both the scalloped shell and the shell of revolution it is possible to find a solution  $\Psi_p$  that meets requirements (36)-(38). In the shell of revolution, the functions  $f_m$  form a set of orthogonal trigonometric functions. The coefficients  $A_m$  can then be readily determined, from this orthogonality property, to prescribe appropriate edge forces at  $\rho = 1$ . Along this edge the force  $n_r$  due to the particular solution  $\Psi_p$  is equal to  $(1 - \rho_0^2)/4\mu$ , and the dimensionless sum of its vertical components along this edge is a downward force of magnitude  $\theta_0(1 - \rho_0^2)$ . The sum of the vertical components of the force  $n_r$  due to the homogeneous solution  $\Psi_H$  vanishes along this edge. This implies that a proper boundary condition at  $\rho = 1$  consists of a distribution of the force  $n_r$ , which has the same vertical resultant as that due to the particular solution. Two such distributions are shown in figures 10(a) and 10(b). For the scalloped model, on the other hand, it is not necessary to follow the same pattern because the corresponding homogeneous solutions do contribute a vertical resultant. In this case, however, the coefficients  $A_m$  have to be determined by numerical techniques, with resulting numerical difficulties if  $N$  is large and if a large number of terms of the homogeneous solution are needed to prescribe vanishing edge force  $n_r$  at  $\rho = 1$ . However, if  $\beta$  is close to  $\beta_{cr}$ , then only a few terms of the homogeneous solution would be adequate to meet requirement (39). This is true because in the scalloped model, as will be seen later, the forces  $n_r$  decrease as  $\beta$  increases and become very small at the base when  $\beta$  is close

to  $\beta_{cr}$ . In the shell of revolution, on the other hand, these forces increase toward the base and become almost constant in the lower parts of the shell.

The membrane forces  $n_r$ ,  $n_\theta$ ,  $n_{r\theta}$  and the rope tension  $T$  presented in figures 11-14 have been obtained by means of the first 25 terms of each of the series in  $x$  in expressions (43) - (46). The broken lines in these figures represent the membrane forces in a similar shell of revolution subjected to the boundary condition in figure 10(b) for  $\xi = 0.1$ . It can be seen from these figures that, for equilibrium of the shell, all three stress resultants  $n_r$ ,  $n_\theta$ ,  $n_{r\theta}$  are necessary. For the particular parameters chosen the force  $n_r$  decreases toward the edge  $\rho = 1$ . This drop in  $n_r$  is more noticeable along the central meridian than along the edge  $\theta = \theta_0$  (fig. 12). The hoop force  $n_\theta$  at a given radius (fig. 13) remains nearly constant although its magnitude varies with the radius and reaches a peak value at the edge  $\rho = 1$ . The shear forces are relatively low, except in the lower half of the shell near the edge  $\theta = \theta_0$ . The rope tension  $T$  (fig. 14) has a maximum value at the base ( $\rho = 1$ ) and decreases steadily toward the apex.

It is interesting to note how the membrane forces in the scalloped shell differ from those in a similar shell of revolution (figs. 11 and 12). It can be seen that the forces  $n_r$  in the scalloped shell are significantly lower than those in the shell of revolution. The forces  $n_\theta$  are also lower but not as significantly as the forces  $n_r$ . The shear force  $n_{r\theta}$  in the shell of revolution vanishes at  $\theta = \theta_0$ , whereas in the scalloped shell a relatively low but nonvanishing shear force is necessary at this edge. The behavior of the forces  $n_r$ ,  $n_\theta$  in the shell of revolution along  $\theta = \theta_0$  is also worth noting: These forces have high magnitudes in the neighborhood of the lower corners, and  $n_\theta$  even changes sign and becomes compressive.

It should be mentioned, at this point, that the solution  $k/2\mu \log(\rho\sqrt{1+x^2})$ , with  $k = 0.0017$  in the particular example, corresponds to a downward load of magnitude  $0.35\pi b^2 p$  at the apex. In figure 8, the ropes, but not the scallops, are continued to the apex. Prescribing a value for  $k$  therefore amounts to assuming a certain amount of tension in these ropes at  $\rho = \rho_0$ . In the particular example considered, if  $k > 0.0017$  the edge forces  $n_r$  at  $\rho = \rho_0$  due to  $\Psi_p$  would be compressive, while if  $k < 0.0017$  these forces would be tensile. In either case, appropriate values for  $n_r$  would have to be prescribed along this edge by means of the homogeneous solutions associated with the negative eigenvalues.

It was mentioned earlier in this section that in order to meet the tensile requirement (40), the parameter  $\beta$  should be less than  $\beta_{cr}$ . This can be illustrated in figure 15 where membrane forces due to the dominant solution  $\Psi_p$  are plotted along the central meridian for different values of  $\beta$ . The constant  $k$  in each case has been chosen equal to  $k_{cr}$  to meet requirement (38). This figure shows that when  $\beta$  is very small the membrane forces approach those in a corresponding shell of revolution ( $\beta = 0$ ). However, as  $\beta$  increases the stress resultant  $n_r$  decreases markedly, and, for  $\beta = 0.6$ , even changes sign and becomes compressive in the region  $\rho \geq 0.75$ . The hoop force  $n_\theta$  decreases also, although not as significantly as the meridional force  $n_r$ . It can be seen that when  $\beta$  is less than 0.5, the

shell (and a corresponding parachute) could support the applied uniform pressure by means of tensile and shear forces alone.

## SCOPE AND LIMITATIONS

The stress function approach is valid as long as there exists a one-to-one correspondence between points of the middle surface and their projections on a reference plane. The scalloped paraboloids (eq. (9)) meet this requirement. The mathematical approach in appendix A for finding this stress function  $\Psi$  relies on two important conditions. First, the differential equation and the boundary conditions must be such that the method of separation of variables can be applied. Second, the solutions involving the variable  $x$  must be obtainable in the form of an infinite series in powers of  $x$ . These requirements are fulfilled in the problems considered so far. It is of interest to mention other problems where these requirements may be met.

Consider, for example, the more general class of surfaces

$$Z = Ar^n(1 + \beta\theta^2) \quad (47)$$

of which the scalloped paraboloids constitute a special case. These surfaces meet the above requirements for application of the stress function approach. When such shells are subjected to uniform normal pressure, the stress function  $\Psi$  must satisfy the differential equation.

$$\begin{aligned} & \left( \frac{n}{2} + \beta + \frac{n}{2} x^2 \right) \frac{\partial^2 \Psi}{\partial \rho^2} - 2(n-1)\beta x \frac{1}{\rho} \frac{\partial^2 \Psi}{\partial \rho \partial x} + \frac{1}{2} n(n-1)(1+x^2) \frac{\beta}{\rho^2} \frac{\partial^2 \Psi}{\partial x^2} \\ & + \frac{1}{2} n(n-1)(1+x^2) \frac{1}{\rho} \frac{\partial \Psi}{\partial \rho} + 2(n-1)\beta x \frac{1}{\rho^2} \frac{\partial \Psi}{\partial x} \\ & = \frac{1}{2\mu} \rho^{2-n} + \mu \rho^n \left[ \frac{n^3}{n+1} + \left( n^2 \frac{2n+1}{n+1} + 3\beta \right) x^2 + n^2 x^4 \right] \end{aligned} \quad (48)$$

where the membrane forces are related to the stress function  $\Psi$  as follows:

$$\left. \begin{aligned} n_r &= \frac{1}{\rho} \frac{\partial \Psi}{\partial \rho} + \frac{\beta}{\rho^2} \frac{\partial^2 \Psi}{\partial x^2} - \mu \rho^n \left( \frac{n}{n+1} + x^2 \right) \\ n_\theta &= \frac{\partial^2 \Psi}{\partial \rho^2} - \mu \rho^n x^2 \\ n_{r\theta} &= \sqrt{\beta} \left( \frac{1}{\rho^2} \frac{\partial \Psi}{\partial x} - \frac{1}{\rho} \frac{\partial^2 \Psi}{\partial \rho \partial x} \right) \end{aligned} \right\} \quad (49)$$



It can be verified that the boundary conditions, similar to those for the two cases considered, are such that the method of appendix A can be applied to equation (48) to obtain solution  $\Psi$  in the form:

$$\Psi(\rho, x) = \frac{1}{2\mu} \rho^\alpha F_\alpha(x) + \mu \rho^\gamma F_\beta(x) + \frac{k}{2\mu} \rho^\delta F_\gamma(x) + \Psi_H(\rho, x) \quad (50)$$

where

$$\left. \begin{aligned} \alpha &= 4 - n \\ \gamma &= n + 2 \\ \delta &= 2 - n \end{aligned} \right\} \quad (51)$$

$$k \begin{cases} = 0 & \text{for a single scallop} \\ \neq 0 & \text{for a parachute model} \end{cases}$$

When  $\delta = 0$  (or  $n = 2$ ) the third term of (50) is replaced by  $k/2\mu \log(\rho\sqrt{1+x^2})$ .

It should be pointed out that it is not generally possible to find a solution in the form of equation (50) if any of the indices  $\alpha, \gamma, \delta$  is equal to an eigenvalue of the corresponding eigenvalue problem. For example,  $\lambda = 1$  happens to be an eigenvalue for all  $n$ ; hence, difficulties may be encountered when  $n = 1$  and  $n = 3$ . In order to predict whether a solution in the form of equation (50) does or does not exist for a given problem, it is necessary to investigate each individual case further. It is interesting to note that since the shells corresponding to  $n > 2$  become relatively flat in the polar regions, the membrane forces must be high in these regions in order to balance the applied normal pressure. For such cases the structure would require additional reinforcement in the upper regions.

#### CONCLUDING REMARKS

In the preceding sections it has been shown that the stress function approach can be successfully used in solving problems of scalloped paraboloids. It has been further demonstrated that the surface parameters associated with these problems may profoundly affect the application of the scalloped shell - particularly where a compressionless state is desired. The two scalloped structures considered in detail in this report are characterized by the parameters  $N, \mu, \rho_0, \beta$ , and defined by equation (9). It has been shown for the parachute model that for a given large  $N$  and given values of the parameters  $\rho_0, \mu$ , it is possible to use  $k = k_{cr}$  in the particular solution  $\Psi_p$  to determine the maximum allowable bulge parameter  $\beta_{cr}$ , beyond which the meridional stress could become compressive. It was found in the particular example considered that for given  $N (= 12)$  and  $\rho_0 (= 0.1)$ , the greater the value of  $\mu$ , the smaller the value of  $\beta_{cr}$ . It would be useful to carry this

investigation further and plot relationships between  $\mu$  and  $\beta_{cr}$  for different sets of  $\rho_0$  and  $N$ . Such plots could serve as a useful aid in the design of parachute-type structures.

As mentioned earlier in this report, the only difference between the forms of the solutions for the two cases considered is the term  $k/2\mu \log(\rho\sqrt{1+x^2})$ , which is singular at the apex. For the single scallop, this term is absent. For the parachute model shown in figure 8 this term is used to prescribe a certain amount of tension in the ropes in the region  $\rho < \rho_0$ . Solutions of this type may be useful in other aspects of parachute analysis, as well.

In the case of the single scallop the character of the stresses does not seem to be radically affected by the magnitude of the bulge parameter  $\beta$ ; but such is not the case with the parachute type structure, as can be seen in figure 15. The latter structure, when designed to the critical  $\beta$ , has a lower hoop stress and a much lower meridional stress than the corresponding shell of revolution. In comparison with shells of revolution, indications are that the scalloped shell may be an efficient structural form warranting further study. It would be useful indeed to extend the analysis to include bending, deformation, and material properties, and to consider the scalloped shell for other structural applications such as pressure vessel bulkheads.

Ames Research Center

National Aeronautics and Space Administration

Moffett Field, Calif., 94035, May 7, 1968

124-08-06-01-00-21

## APPENDIX A

### THE SOLUTION $\Psi$ FOR THE SINGLE SCALLOP

#### PARTICULAR SOLUTION

Consider the differential equation for the single scallop,

$$L[\Psi(\rho, x)] = F(\rho, x) ; \quad 0 \leq \rho \leq 1 , \quad 0 \leq x \leq x_0 \quad (A1)$$

subject to the boundary condition

$$\left( \frac{\partial^2 \Psi}{\partial \rho^2} - \mu \rho^2 x^2 \right) = 0 \quad \text{at} \quad x = x_0 \quad (A2)$$

The operator  $L$  and the function  $F$  are defined in equations (16) and (17).  
Let

$$\Psi(\rho, x) = \Psi_p(\rho, x) + \Psi_H(\rho, x) \quad (A3)$$

where  $\Psi_p$  satisfies equation (A1) and the boundary condition (A2). If  $\Psi_p$  is assumed in the separated form,

$$\Psi_p(\rho, x) = \frac{1}{2\mu} \rho^2 F_\alpha(x) + \mu \rho^4 F_\beta(x) \quad (A4)$$

then  $F_\alpha, F_\beta$  must satisfy the equations

$$\beta(1 + x^2)F_\alpha'' - 2\beta x F_\alpha' + 2(2 + \beta + 2x^2)F_\alpha = 1 \quad (A5)^1$$

$$\beta(1 + x^2)F_\beta'' - 6\beta x F_\beta' + 4(4 + 3\beta + 4x^2)F_\beta = \frac{8}{3} + \left(3\beta + \frac{20}{3}\right)x^2 + 4x^4$$

$$0 \leq x \leq x_0 \quad (A6)$$

and the boundary conditions

$$F_\alpha(x_0) = 0 \quad (A7)$$

$$F_\beta(x_0) = \frac{x_0^2}{12} \quad (A8)$$

---

<sup>1</sup>When used as function superscripts, the primes denote appropriate differentiation with respect to  $x$ .

Solutions for  $F_\alpha(x)$ ,  $F_\beta(x)$  can be found in the form of a convergent series containing terms in even powers of  $x$  as follows:

$$F_\alpha(x) = f_\alpha(x) + \mu_\alpha g_\alpha(x) \quad (A9)$$

$$F_\beta(x) = f_\beta(x) + \mu_\beta g_\beta(x) \quad (A10)$$

where  $\mu_\alpha$ ,  $\mu_\beta$  are constants to be determined and

$$f_\alpha(x) = \sum_{0,2,4,\dots} \alpha'_n x^n \quad (A11)$$

$$f_\beta(x) = \sum_{0,2,4,\dots} \beta'_n x^n \quad (A12)$$

$$g_\alpha(x) = \sum_{0,2,4,\dots} \alpha''_n x^n \quad (A13)$$

$$g_\beta(x) = \sum_{0,2,4,\dots} \beta''_n x^n \quad (A14)$$

The functions  $f_\alpha$ ,  $f_\beta$  must satisfy the inhomogeneous equations (A5) and (A6), while  $g_\alpha$ ,  $g_\beta$  must satisfy the corresponding homogeneous equations. The coefficients  $\alpha'_n$ ,  $\alpha''_n$ ,  $\beta'_n$ ,  $\beta''_n$  can then be obtained from the resulting recurrence relationships,

$$\alpha'_{n+2} = \frac{1}{\beta(n+2)(n+1)} \left\{ \gamma_n - [n(n-3)\beta + 2(2+\beta)]\alpha'_n - 4\alpha'_{n-2} \right\} \quad (A15)$$

$$\beta'_{n+2} = \frac{1}{\beta(n+2)(n+1)} \left\{ \gamma'_n - [n(n-7)\beta + 4(4+3\beta)]\beta'_n - 16\beta'_{n-2} \right\} \quad (A16)$$

$$\alpha''_{n+2} = -\frac{1}{\beta(n+2)(n+1)} \left\{ [n(n-3)\beta + 2(2+\beta)]\alpha''_n + 4\alpha''_{n-2} \right\} \quad (A17)$$

$$\beta''_{n+2} = -\frac{1}{\beta(n+2)(n+1)} \left\{ [n(n-7)\beta + 4(4+3\beta)]\beta''_n + 16\beta''_{n-2} \right\} \quad (A18)$$

for  $n = 0, 2, 4, \dots$

where

$$\left. \begin{aligned} \gamma_0 &= 1, & \gamma_n &= 0 & \text{for } n > 0 \\ \gamma'_0 &= \frac{8}{3}, & \gamma'_2 &= 3\beta + \frac{20}{3}, \\ \gamma'_4 &= 4, & \gamma'_n &= 0 & \text{for } n > 4 \\ \alpha'_n &= 0 & \text{for } n \leq 0; & \beta'_n &= 0 & \text{for } n \leq 0 \\ \alpha''_0 &= \beta''_0 = 1; & \alpha''_n &= \beta''_n = 0 & \text{for } n < 0 \end{aligned} \right\} \quad (A19)$$

and

The constants of integration  $\mu_\alpha, \mu_\beta$  in (A9) and (A10) are obtained by requiring that  $F_\alpha, F_\beta$  satisfy conditions (A7) and (A8), so that

$$\mu_\alpha = \frac{- \sum_{0,2,4,\dots} \alpha'_n x_0^n}{\sum_{0,2,4,\dots} \alpha''_n x_0^n} \quad (A20)$$

$$\mu_\beta = \frac{(x_0^2/12) - \sum \beta'_n x_0^n}{\sum \beta''_n x_0^n} \quad (A21)$$

Defining the coefficients  $\alpha_n, \beta_n$  by

$$\alpha_n = \alpha'_n + \mu_\alpha \alpha''_n \quad (A22)$$

$$\beta_n = \beta'_n + \mu_\beta \beta''_n \quad n = 0, 2, 4, \dots \quad (A23)$$

The solutions  $F_\alpha$  and  $F_\beta$  can be finally written in the form:

$$F_\alpha(x) = \sum_{n=0,2,4,\dots} \alpha_n x^n \quad (A24)$$

$$F_\beta(x) = \sum_{n=0,2,4,\dots} \alpha_n x^n \quad (A25)$$

## HOMOGENEOUS SOLUTION

Consider a homogeneous solution

$$\Psi_{Hm}(\rho, x) = \rho^{\lambda_m} f_m(x)$$

which satisfies

$$L(\Psi_{Hm}) = 0 \quad (A26)$$

and the boundary conditions

$$\frac{\partial^2}{\partial \rho^2} \Psi_{Hm}(\rho, x) = 0 \quad \text{at } x = x_0 \quad (A27)$$

The function  $f_m(x)$ , then, must satisfy the equation

$$\beta(1 + x^2)f_m'' - 2\beta(\lambda_m - 1)xf_m' + \lambda_m[\beta(\lambda_m - 1) + \lambda_m(1 + x^2)]f_m = 0 \quad (A28)$$

subject to the condition

$$\lambda_m(\lambda_m - 1)f_m(x_0) = 0 \quad \text{at } x = x_0 \quad (A29)$$

A nontrivial solution for  $f_m(x)$  exists only when  $\lambda_m$  equals an eigenvalue of the problem defined by equations (A28) and (A29). The values  $\lambda_m = 0$  and  $\lambda_m = 1$  are obviously two eigenvalues. However, the corresponding homogeneous solutions make no contribution to the membrane forces  $n_r$ ,  $n_\theta$ ,  $n_{r\theta}$ . The eigenvalues of interest, therefore, are associated with the condition

$$f_m(x_0) = 0 \quad (A30)$$

It should be observed that the solution for  $f_m$ , when one exists, can be obtained through the method of infinite series, that is,  $f_m(x)$  may be expanded in the form,

$$f_m(x) = \sum_{n=0,2,4,\dots} C_{m,n} x^n \quad (A31)$$

where

$$C_{m,0} = 1$$

$$C_{m,n} = 0 \quad \text{for } n < 0$$

and

$$C_{m,n+2} = \frac{-1}{(n+1)(n+2)} \left\{ \left[ n(n+1) - 2n(\lambda_m - 1) + \left( 1 + \frac{1}{\beta} \right) \lambda_m^2 - \lambda_m \right] C_{m,n} + \frac{\lambda_m^2}{\beta} C_{m,n-2} \right\} \quad (A32)$$

for  $n = 0, 2, 4, \dots$

Equation (A31) can be applied to (A30) to obtain an infinite series in powers of  $\lambda_m$ . The zeroes of this infinite series are the required eigenvalues. From a practical standpoint, the leading eigenvalues can be found by truncating such a series after a finite number of terms and then finding the roots of the resulting polynomial in  $\lambda_m$ . In the present work, it was found that

for large  $N(= \pi/\theta_0)$  the polynomial approach gives convergent values only for the first one or two zeroes of the infinite series. A more satisfactory approach in this case has been found to be the method of interpolation or the false position method (ref. 9). It must be mentioned, however, that this method is to be applied to equation (A30) in a special way and not to the truncated polynomial. The process essentially consists of selecting a set of values for  $\lambda_m$  at chosen fixed intervals, obtaining the coefficients  $C_{m,n}$  from (A32), and using these  $C_{m,n}$  in (A31) to evaluate each  $f_m(x_0)$ . The approximate zeroes of (A29) are then easily located and it is only necessary to repeat the entire process a suitable number of times in order to converge to suitably accurate roots. In order to use this approach most effectively, it is advantageous to have prior information about the character of the eigenvalues  $\lambda_m$ . In this connection the following discussion will be of interest.

If, instead of using the form (A31),  $f_m(x)$  is expressed in the following form:

$$f_m(x) = (1 + x^2)^{\frac{\lambda_m - 1}{2}} u_m(x) \quad (A33)$$

then it can be verified that  $u_m$  must satisfy

$$u_m'' + \left[ \frac{\lambda_m^2 - 1}{(1 + x^2)^2} + \frac{\lambda_m^2}{\beta} \right] u_m = 0 \quad (A34)$$

$$u_m(x_0) = 0 \quad (A35)$$

Furthermore, if  $\lambda_m$  is a complex eigenvalue and  $u_m$  the corresponding complex eigenfunction, then their complex conjugates  $\bar{\lambda}_m, \bar{u}_m$  also satisfy equations (A34) and (A35).

Using  $u_m, \bar{u}_m$  in Green's first formula (ref. 10)

$$\int_0^{x_0} u_m'' \bar{u}_m dx = (u_m' \bar{u}_m)_0^{x_0} - \int_0^{x_0} u_m' \bar{u}_m' dx \quad (A36)$$

and realizing that  $u_m(x_0) = 0$  and (because of symmetry)  $u_m'(0) = 0$ , equation (A36) reduces to

$$\int_0^{x_0} u_m'' \bar{u}_m dx = - \int_0^{x_0} u_m' \bar{u}_m' dx \quad (A37)$$

Substituting for  $u_m''$  from equation (A34) and rearranging yields

$$\lambda_m^2 = \frac{\int_0^{x_0} u_m' \bar{u}_m' dx + \int_0^{x_0} \frac{1}{(1+x^2)^2} u_m \bar{u}_m dx}{\int_0^{x_0} \left[ \frac{1}{(1+x^2)^2} + \frac{1}{\beta} \right] u_m \bar{u}_m dx} \quad (A38)$$

where  $\beta > 0$  by definition.

It is evident from the above expression that, since  $u_m$  is a nontrivial solution,  $\lambda_m^2$  must always be positive definite. Hence, the eigenvalues are always real, occurring in pairs of positive and negative values of equal magnitudes. Consequently, the homogeneous solution  $\Psi_H$  can be written as

$$\Psi_H(\rho, x) = \sum_{m=1,2,3,\dots} \left[ A_m \rho^{\lambda_m} f_m(x) + B_m^{-\lambda_m} g_m(x) \right] \quad (A39)$$

where the functions  $f_m, g_m$  correspond to the eigenvalues  $+\lambda_m$  and  $-\lambda_m$ , respectively. The function  $f_m$  is obtainable in the form defined in equation (A31), and  $g_m$  is obtainable in the form

$$g_m(x) = \sum_{n=0,2,4,\dots} D_{m,n} x^n \quad (A40)$$

where the coefficients  $D_{m,n}$  can be generated from the recurrence relation (A32) by means of the negative value  $-\lambda_m$ . The stress function can then be written as

$$\begin{aligned} \Psi(\rho, x) = & \frac{1}{2\mu} \rho^2 \sum_{n=0,2,4,\dots} \alpha_n x^n + \mu \rho^4 \sum_{n=0,2,4,\dots} \beta_n x^n \\ & + \sum_{m=1,2,3,\dots} A_m \rho^{\lambda_m} \sum_{n=0,2,4,\dots} C_{m,n} x^n \\ & + \sum_{m=1,2,3,\dots} B_m \rho^{-\lambda_m} \sum_{n=0,2,4,\dots} D_{m,n} x^n \end{aligned} \quad (A41)$$

The homogeneous solutions associated with the negative eigenvalues tend to infinity as  $\rho$  approaches zero. Hence, the coefficients  $B_m$  associated with these solutions must be chosen to be zero if  $\rho = 0$  is to be an included point of the domain. If the domain is terminated at an inner boundary  $\rho = \rho_0$  (corresponding to  $r = b$ ), then the coefficients  $B_m$  may be different



from zero, and their values would have to be determined by resorting to an appropriate numerical technique, such as approximation in the mean, together with an iterative scheme.

#### THE SOLUTION $\Psi$ FOR THE PARACHUTE TYPE STRUCTURE

For the parachute type structure the stress function  $\Psi$  must satisfy equation (36) subject to the condition (37). The solution for this case is similar to that for the single scallop and can be written as

$$\begin{aligned} \Psi(\rho, x) = & \frac{1}{2\mu} \rho^2 \sum_{n=0,2,4,\dots} \alpha_n x^n + \mu \rho^4 \sum_{n=0,2,4,\dots} \beta_n x^n - \frac{k}{2\mu} \log(\rho \sqrt{1+x^2}) \\ & + \sum_{m=1,2,3,\dots} \left[ A_m \rho^{\lambda_m} f_m(x) + B_m \rho^{-\lambda_m} g_m(x) \right] \end{aligned} \quad (A42)$$

The coefficients  $\alpha_n$ ,  $\beta_n$  and the functions  $f_m$ ,  $g_m$  can be found using the approach outlined earlier in this section, where  $\mu_\alpha$  and  $\mu_\beta$  are expressed as follows:

$$\mu_\alpha = \frac{-\frac{1}{2} - \sum_{n=0,2,4,\dots} \left( 3\beta'_n - \frac{2+3\beta}{n+1} \alpha'_n - \frac{2}{n+1} \alpha'_{n-2} \right) x_0^n}{\sum_{n=0,2,4,\dots} \left( 3\beta''_n - \frac{2+3\beta}{n+1} \alpha''_n - \frac{2}{n+1} \alpha''_{n-2} \right) x_0^n} \quad (A43)$$

$$\mu_\beta = \frac{-\frac{2}{3} - \frac{5}{9} x_0^2 - \frac{1}{5} x_0^4 - \sum_{n=0,2,4,\dots} \left( 5\beta'_n - \frac{4+5\beta}{n+1} \beta'_n - \frac{4\beta'_{n-2}}{n+1} \right) x_0^n}{\sum_{n=0,2,4,\dots} \left( 5\beta''_n - \frac{4+5\beta}{n+1} \beta''_n - \frac{4\beta''_{n-2}}{n+1} \right) x_0^n} \quad (A44)$$

The value of the constant  $k$  in (A42) depends on the tension in the ropes in the region  $\rho \leq \rho_0$ .

For the parachute type structure it can be verified that the function  $u_m(x)$  must satisfy the boundary condition

$$(\lambda_m^2 - 1)x_0 u_m(x_0) + (1 + x_0^2)u'_m(x_0) = 0 \quad (A45)$$

where

$$\lambda_m^2 = \frac{\int_0^{x_0} u_m' \bar{u}_m' dx + \int_0^{x_0} \frac{u_m \bar{u}_m dx}{(1+x^2)^2} - \frac{x_0}{1+x_0^2} u_m(x_0) \bar{u}_m(x_0)}{\int_0^{x_0} \left[ \frac{1}{\beta} + \frac{1}{(1+x^2)^2} \right] u_m \bar{u}_m dx - \frac{x_0}{1+x_0^2} u_m(x_0) \bar{u}_m(x_0)} \quad (A46)$$

It follows from equation (A46) that  $\lambda_m^2$  must always be real. The positive definite character of  $\lambda_m^2$  is difficult to establish in this case, but since the solutions corresponding to negative  $\lambda_m^2$  have a rapidly oscillating singularity as  $\rho$  becomes small, the undetermined coefficients associated with these solutions may be chosen appropriately as zero. The eigenvalues of interest, then, are related to the positive values of  $\lambda_m^2$  and are easily obtained by the interpolation procedure described earlier in this appendix.

## APPENDIX B

### MEAN SQUARE APPROXIMATION FOR COEFFICIENTS $A_m$

The method of mean square approximation, used in determining the coefficients  $A_m$  of equations (28) and (41), will be described briefly in this appendix. Consider the case of the single scallop subject to the condition

$$\left. \begin{aligned} \left[ \frac{1}{\rho} \frac{\partial \Psi}{\partial \rho} + \frac{\beta}{\rho^2} \frac{\partial^2 \Psi}{\partial x^2} - \mu \rho^2 \left( \frac{2}{3} + x^2 \right) \right] &= 0 \\ \text{at } \rho &= 1 \end{aligned} \right\} \quad (\text{B1})$$

Using  $\Psi$ , as defined in (28), the above condition can be expressed as

$$\begin{aligned} &\sum_{m=1,2,3,\dots} A_m \sum_{n=0,2,4,\dots} [\lambda_m C_{m,n} + \beta(n+2)(n+1)C_{m,n+2}] x^n \\ &+ \frac{1}{2\mu} \sum_{n=0,2,4,\dots} [2\alpha_n + \beta(n+2)(n+1)\alpha_{n+2}] x^n \\ &+ \mu \sum_{n=0,2,4,\dots} [4\beta_n + \beta(n+2)(n+1)\beta_{n+2}] x^n - \mu \left( \frac{2}{3} + x^2 \right) = 0 \end{aligned} \quad (\text{B2})$$

or, more concisely, as

$$\sum_{m=1,2,3,\dots} A_m g_m(x) - y(x) = 0 \quad (\text{B3})$$

where

$$\left. \begin{aligned} g_m(x) &= \sum_{n=0,2,4,\dots} a_{m,n} x^n \\ y(x) &= \sum_{n=0,2,4,\dots} \mu_n x^n \end{aligned} \right\} \quad (\text{B4})$$

The coefficients  $a_{m,n}$ ,  $\mu_n$  in equation (B4) are defined by

$$\left. \begin{aligned} a_{m,n} &= \lambda_m C_{m,n} + \beta(n+2)(n+1)C_{m,n+2} \\ \mu_n &= -\frac{1}{2\mu} [2\alpha_n + \beta(n+2)(n+1)\alpha_{n+2}] \\ &\quad - \mu[4\beta_n + \beta(n+2)(n+1)\beta_{n+2} - \delta_n] \end{aligned} \right\} \quad (B5)$$

where

$$\left. \begin{aligned} \delta_0 &= \frac{2}{3}, \quad \delta_2 = 1 \\ \delta_n &= 0 \quad \text{for } n > 2 \end{aligned} \right\} \quad (B6)$$

The summation in (B3) is an infinite series, which includes correspondingly an infinite number of the undetermined coefficients  $A_m$ . For practical purposes this series is truncated after a suitable number of terms,  $k$ , and the coefficients  $A_m$  are determined to minimize the square of the difference between the sum  $\sum_{m=1,2,\dots,k} A_m g_m(x)$  and the function  $y(x)$  in the interval

$0 \leq x \leq x_0$ . This is the basic principle underlying the technique of mean square approximation (ref. 11). Its application to scalloped paraboloids can be described as follows:

Define

$$R(x) = \sum_{m=1,2,3,\dots,k} A_m g_m(x) - y(x) \quad (B7)$$

and

$$Q = \int_0^{x_0} [R(x)]^2 dx = \int_0^{x_0} \left[ \sum_{m=1,\dots,k} A_m g_m(x) - y(x) \right]^2 dx \quad (B8)$$

For  $Q$  to be minimum the following conditions must be satisfied:

$$\frac{\partial}{\partial A_r} (Q) = 0 \quad \text{for } r = 1, 2, \dots, k \quad (B9)$$

Hence, the condition

$$\int_0^{x_0} [\sum A_m g_m(x) g_r(x)] dx = \int_0^{x_0} y(x) g_r(x) dx \quad r = 1, 2, \dots, k \quad (B10)$$

or, interchanging the order of integration and summation,

$$\sum_{m=1,2,\dots} A_m \int_0^{x_0} g_m(x) g_r(x) dx = \int_0^{x_0} y(x) g_r(x) dx \quad r = 1, 2, \dots, k \quad (B11)$$

Conditions (B11) can be expressed as a set of  $k$  simultaneous equations in unknown  $A_m$ , that is,

$$c_{r,m} A_m = B_r \quad r, m = 1, 2, \dots, k \quad (B12)$$

where

$$c_{r,m} = \int_0^{x_0} g_r(x) g_m(x) dx = \sum_{s=0,2,4,\dots} \sum_{n=0,2,4,\dots} \frac{a_{r,s} a_{m,n} x_0^{s+n+1}}{s+n+1} \quad (B13)$$

$$B_r = \int_0^{x_0} y(x) g_r(x) dx = \sum_{s=0,2,4,\dots} \sum_{n=0,2,4,\dots} \frac{\mu_n a_{r,s}}{n+s+1} x_0^{s+n+1} \quad (B14)$$

for  $r, m = 1, 2, \dots, k$

The unknown coefficients  $A_m$  are determined by solving the simultaneous equations (B12).

The results presented for the two examples have been obtained by the technique just described. When the structure has a boundary at  $\rho = \rho_0$  (corresponding to  $r = b$ ) and the magnitude of the lowest eigenvalue,  $|\lambda_1|$ , is sufficiently high, the homogeneous solutions are such that any disturbance produced at the edge  $\rho = 1$  decays before reaching the edge  $\rho = \rho_0$ . The method given here, then, can be used separately for correcting the value at each of the two boundaries,  $\rho = \rho_0$  and  $\rho = 1$ . In other cases it may be necessary to combine the present approach with an iterative scheme similar to the one described in reference 8.

## REFERENCES

1. Anon.: Performance of and Design Criteria for Deployable Aerodynamic Decelerators. Tech. Rep. ASD-TR-61-579, Wright-Patterson Air Force Base, Ohio, 1963.
2. Jones, R.: On the Aerodynamic Characteristics of Parachutes. Aeronautical Research Council, Reports and Memoranda No. 862, London, June 1923.
3. Duncan, W. J.; Stevens, G. W. H.; and Richards, G. J.: Theory of the Flat Elastic Parachute. Aeronautical Research Council, Reports and Memoranda No. 2118, London, March 1942.
4. Stevens, G. W. H.; and Johns, T. F.: The Theory of Parachutes With Cords Over the Canopy. Aeronautical Research Council, Reports and Memoranda No. 2320, London, July 1942.
5. Heinrich, H. G.; and Jamison, L. R., Jr.: Parachute Stress Analysis During Inflation and at Steady State. J. Aircraft, vol. 3, no. 1, Jan.-Feb. 1966, pp. 52-58.
6. Topping, A. D.; Marketos, J. D.; and Costakos, N. C.: A Study of Canopy Shapes and Stresses for Parachutes in Steady Descent. WADC Tech. Rep. 55-294, Oct. 1955.
7. Flügge, W.: Stresses in Shells. Springer-Verlag, Berlin, 1960.
8. Vyas, Ravindra K.: Cut-Outs in Membrane Shells. Ph.D. Dissertation, Stanford University, March 1966.
9. Scarborough, J. B.: Numerical Mathematical Analysis. Fifth ed., The Johns Hopkins Press, Baltimore, 1962.
10. Berg, P. W.; and McGregor, J. L.: Elementary Partial Differential Equations. Holden-Day, San Francisco, Preliminary edition, 1964.
11. Hildebrand, F. B.: Introduction to Numerical Analysis. McGraw-Hill, 1956.

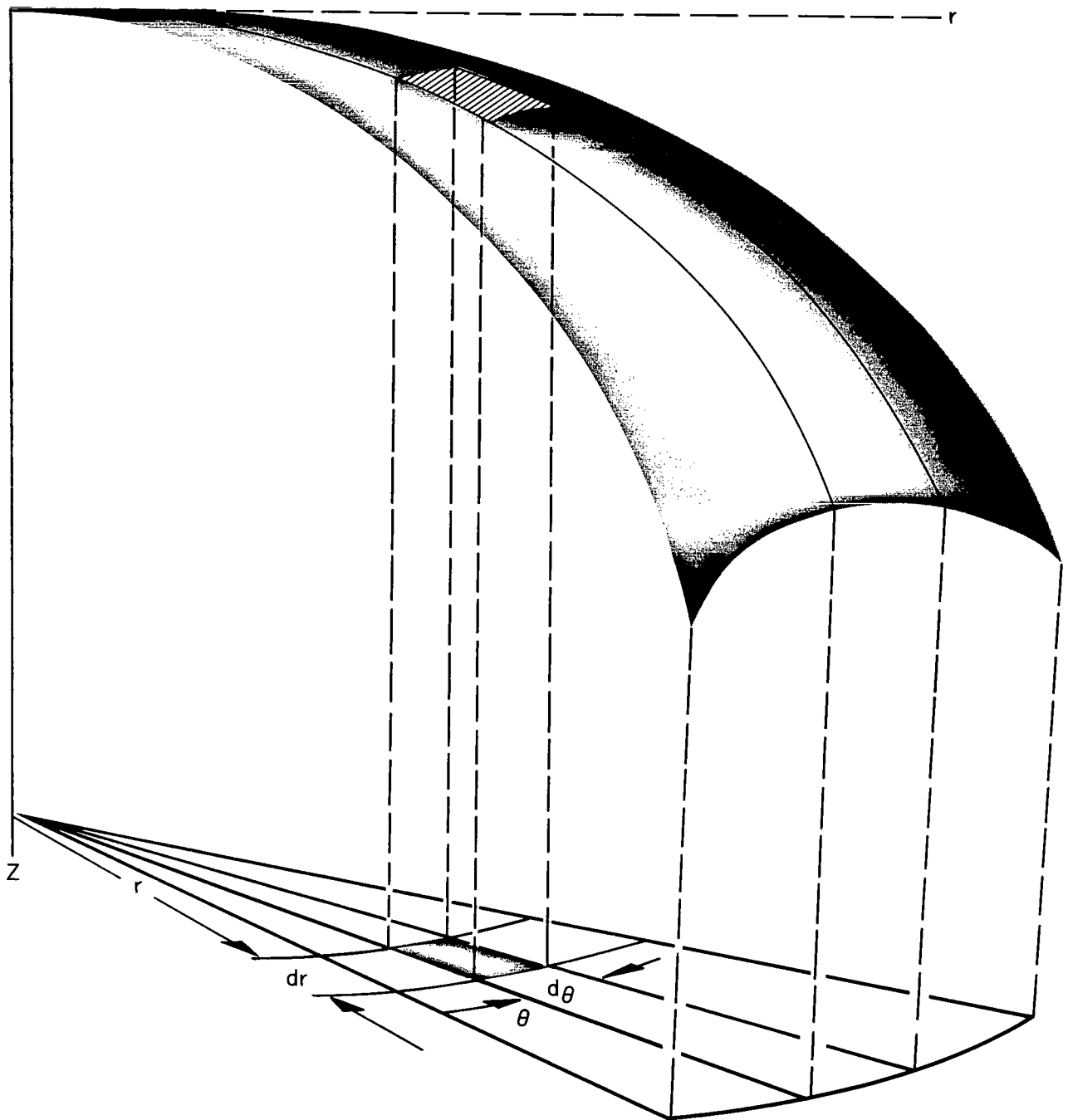


Figure 1.- Middle surface of the shell in cylindrical coordinates.

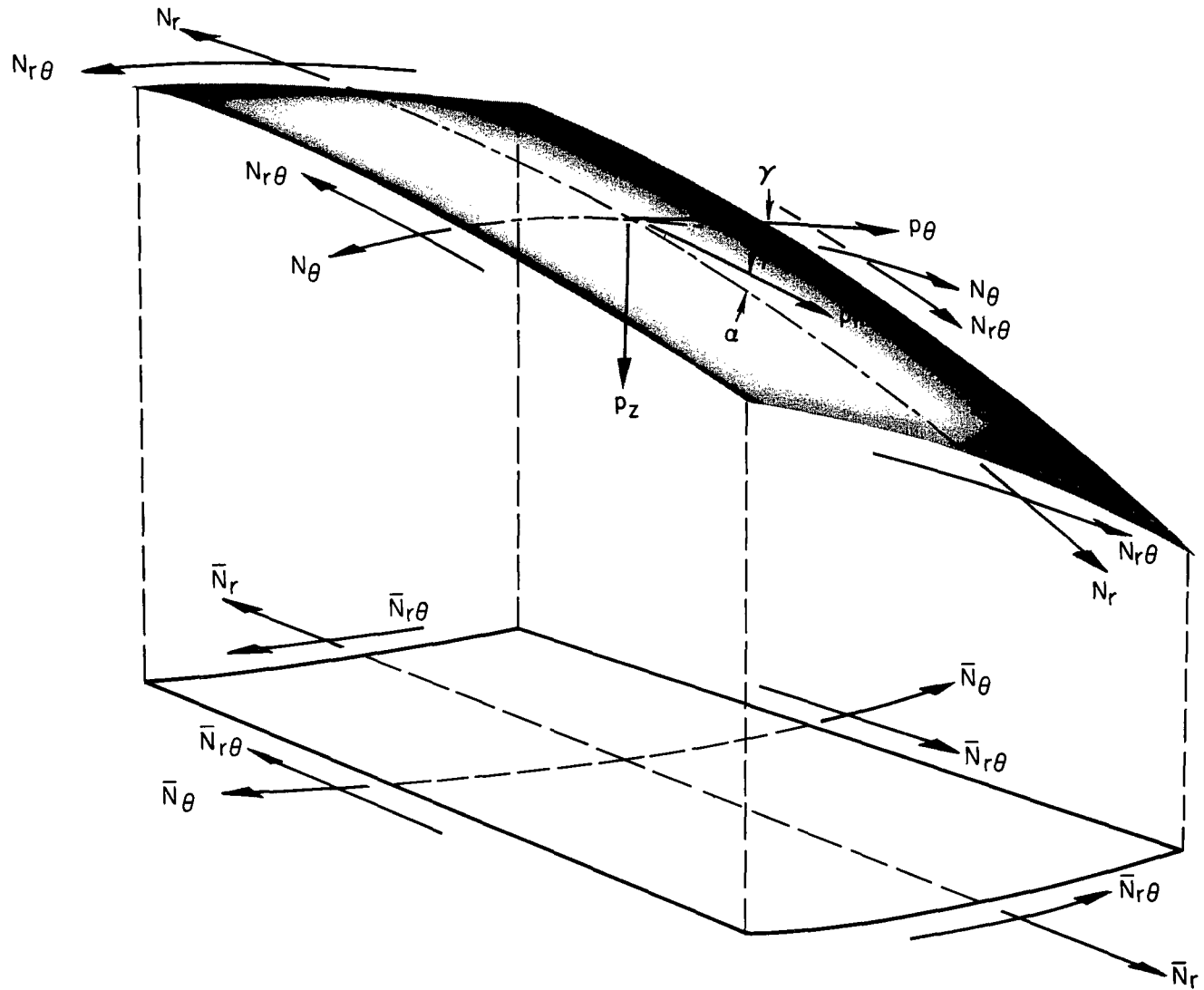


Figure 2.- Shell element.



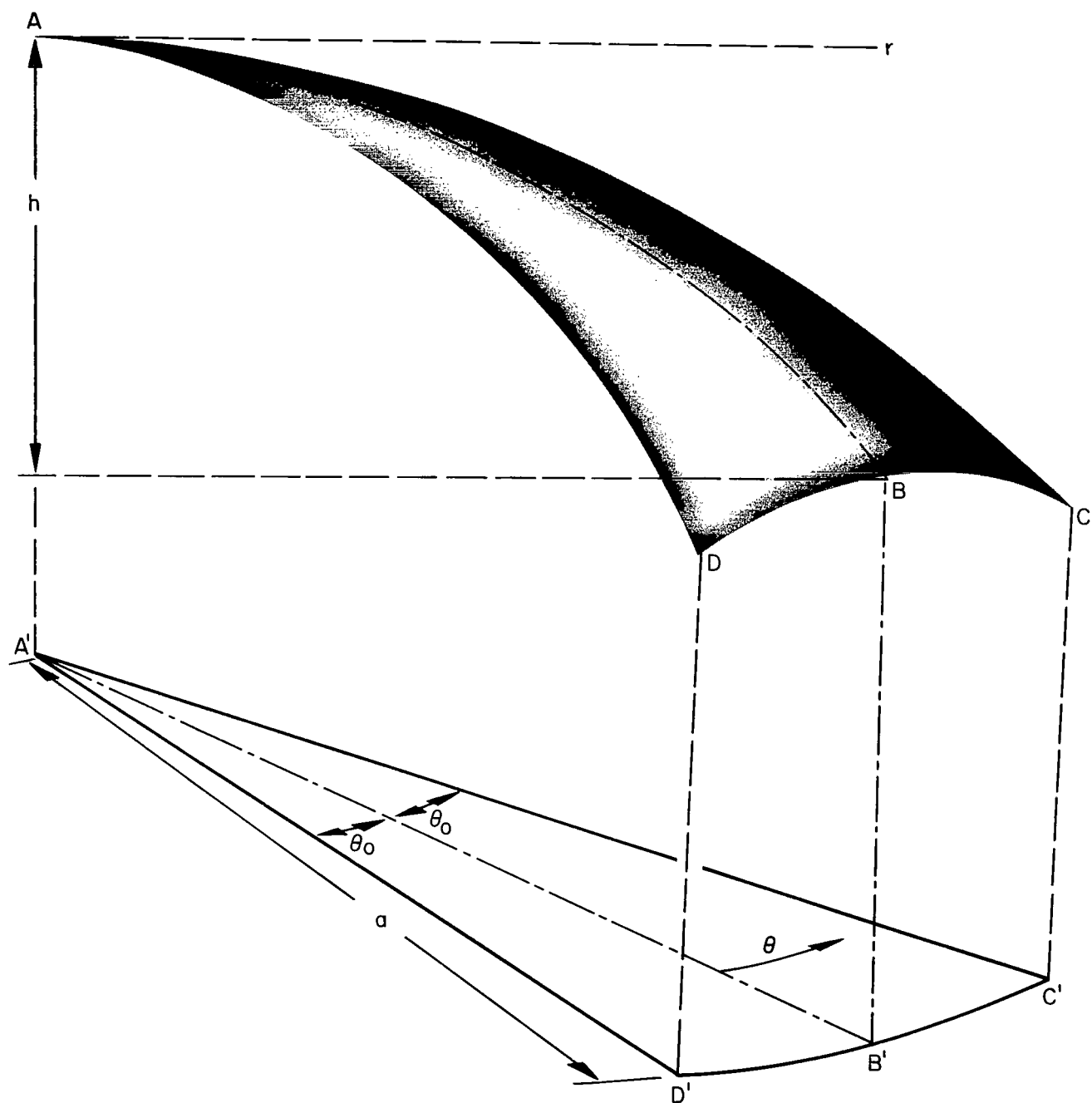


Figure 3.- Middle surface of the single scallop.

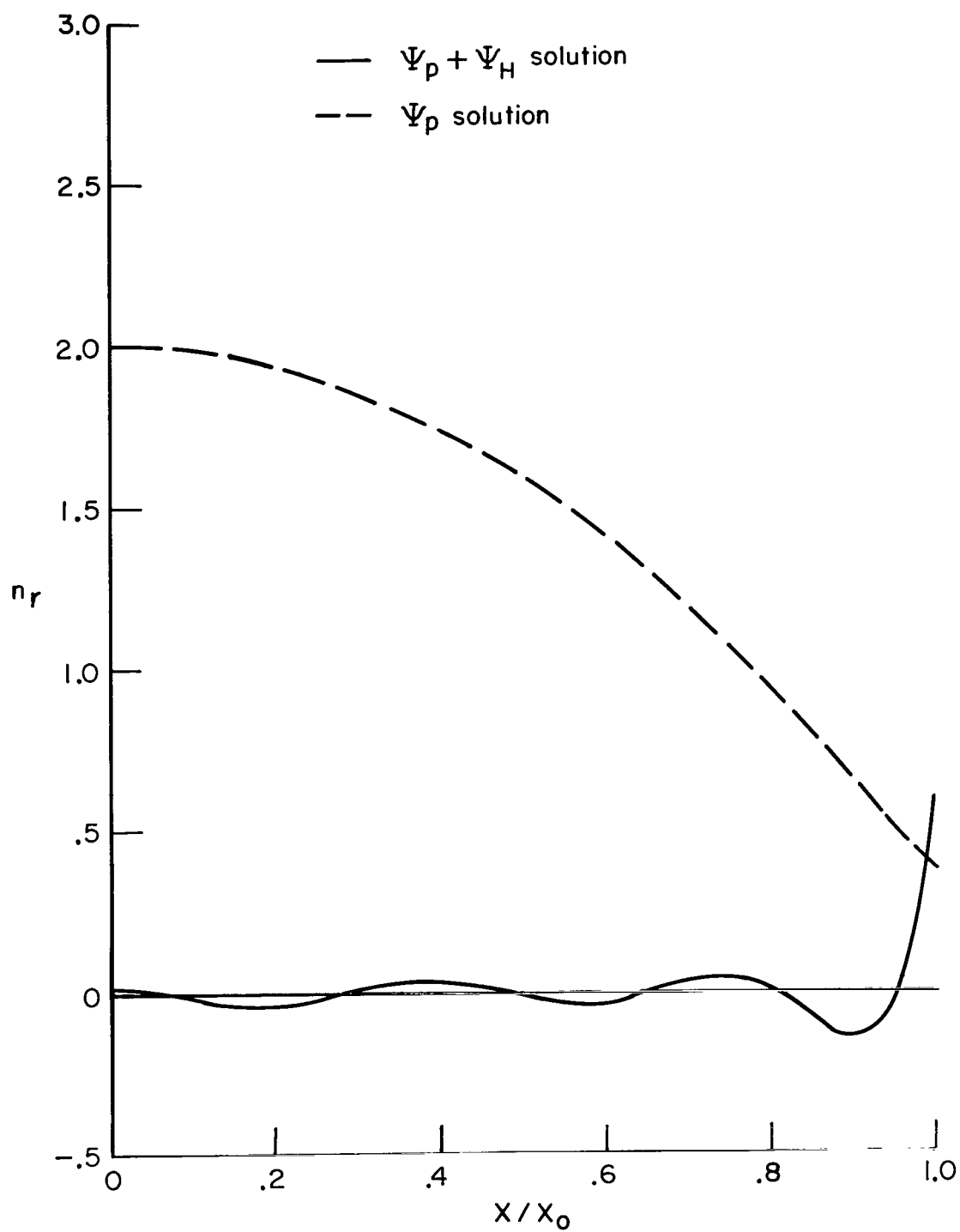


Figure 4.- The single scallop; membrane force  $n_r$  along the edge;  $\rho = 1$ ;  
 $0 \leq x \leq x_0$ .

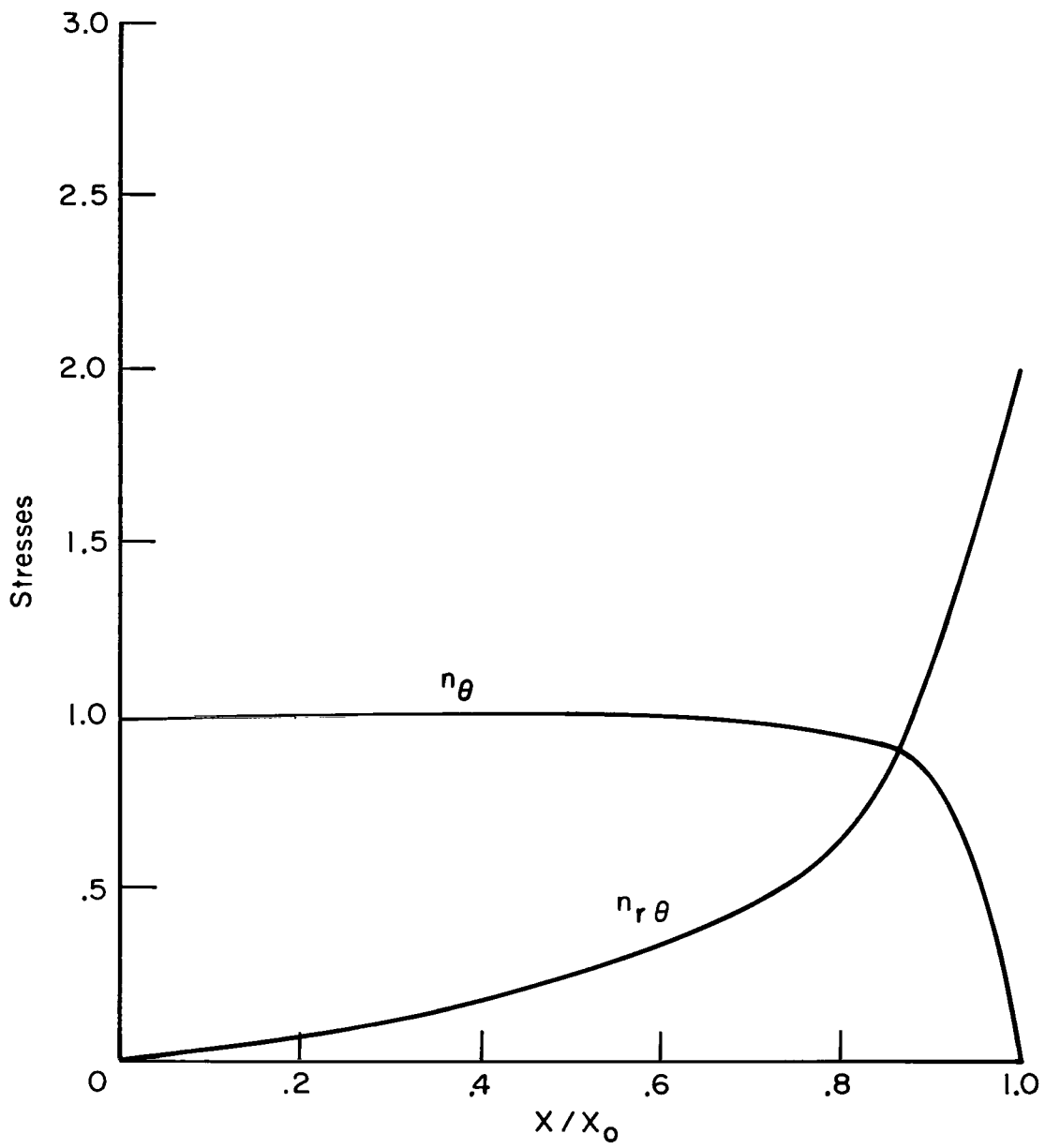


Figure 5.- The single scallop; membrane forces  $n_\theta$ ,  $n_{r\theta}$  along the edge;  $\rho = 1$ ;  
 $0 \leq x \leq x_0$ .

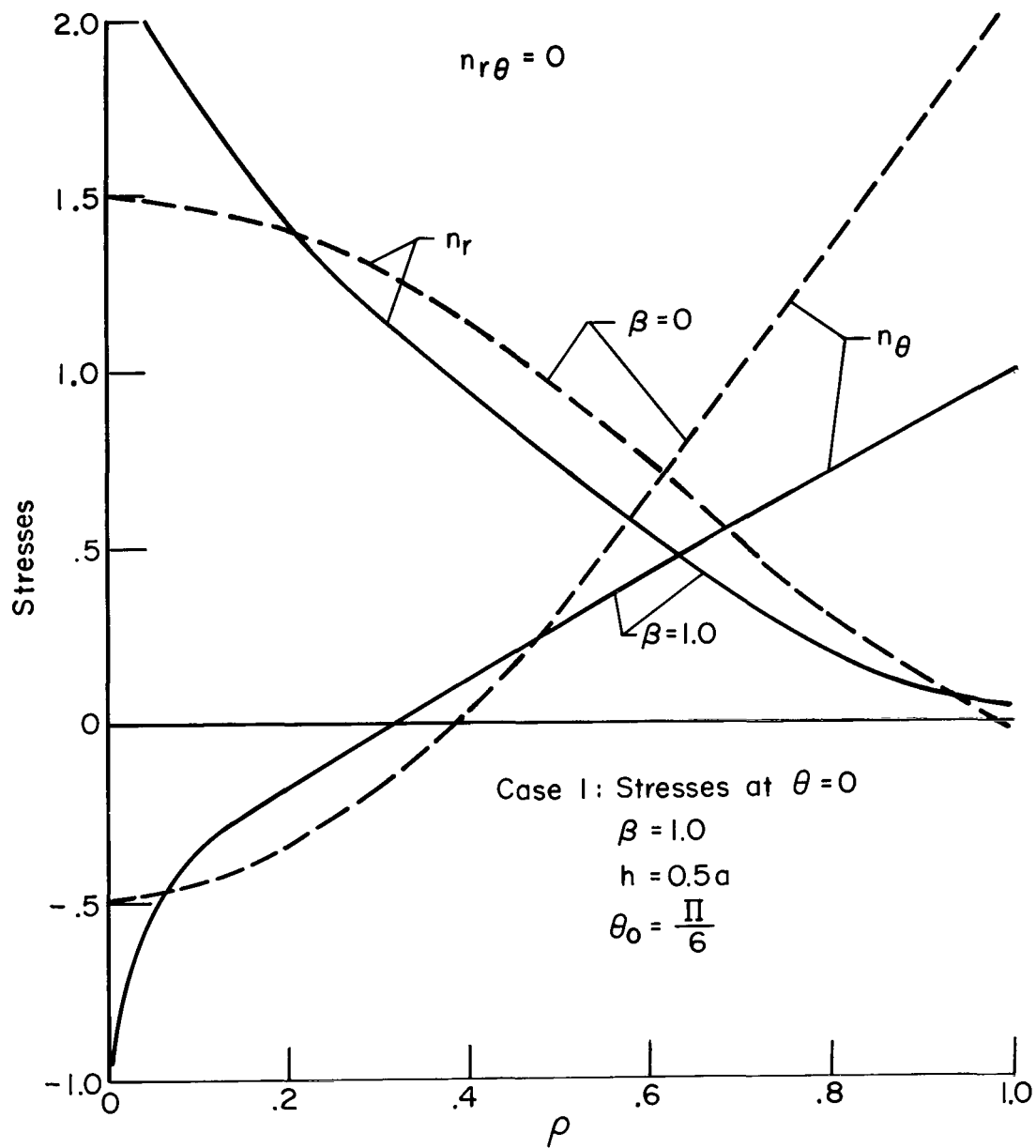


Figure 6.- The single scallop; membrane forces  $n_r, n_\theta$  along the central meridian;  $x = 0$ ;  $0 \leq \rho \leq 1$ ;  $n_{r\theta} = 0$ .

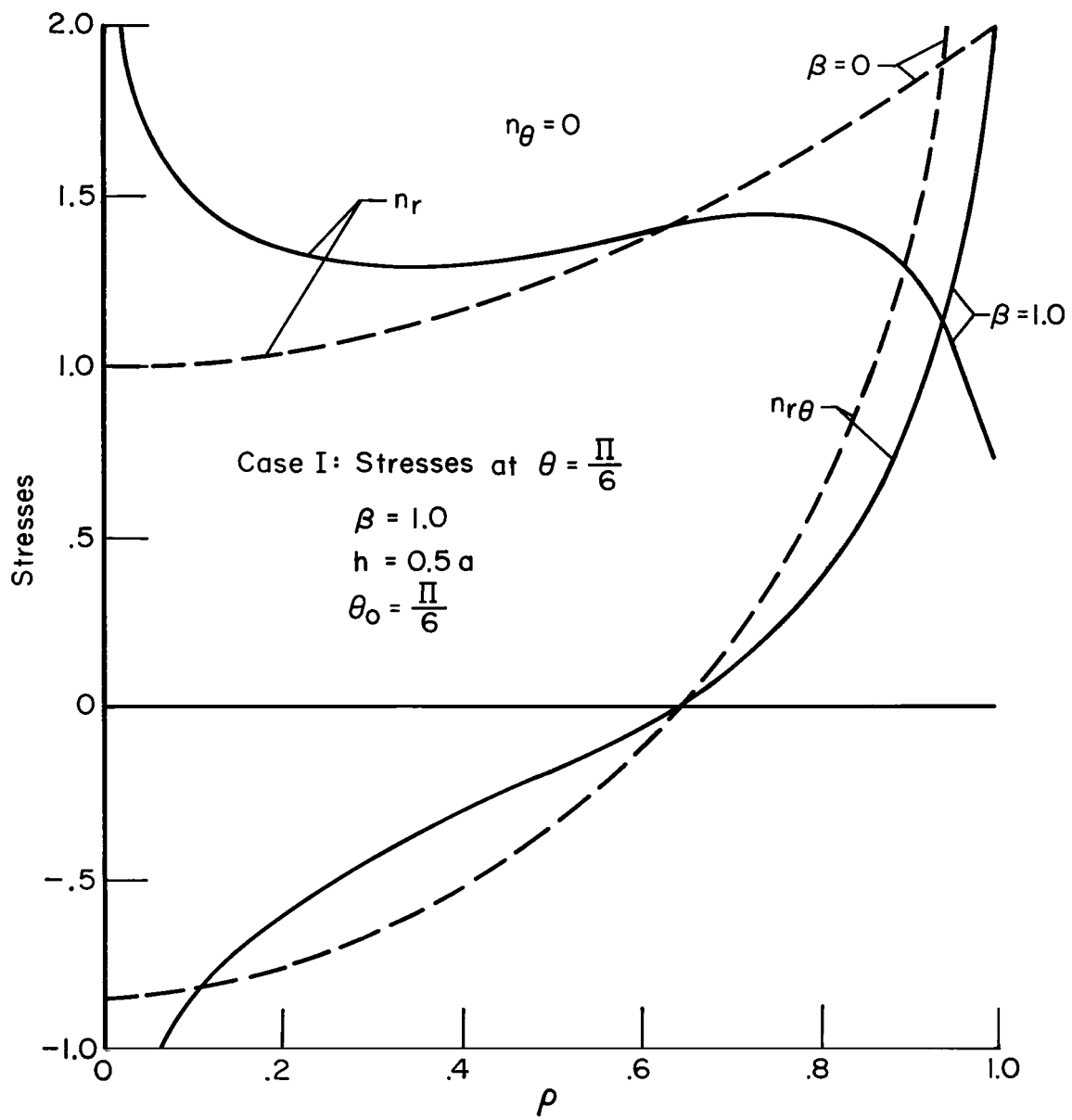


Figure 7.- The single scallop; membrane forces  $n_r$ ,  $n_{r\theta}$  along the edge;  $x = x_0$ ;  $0 \leq \rho \leq 1$ ;  $n_\theta = 0$ .

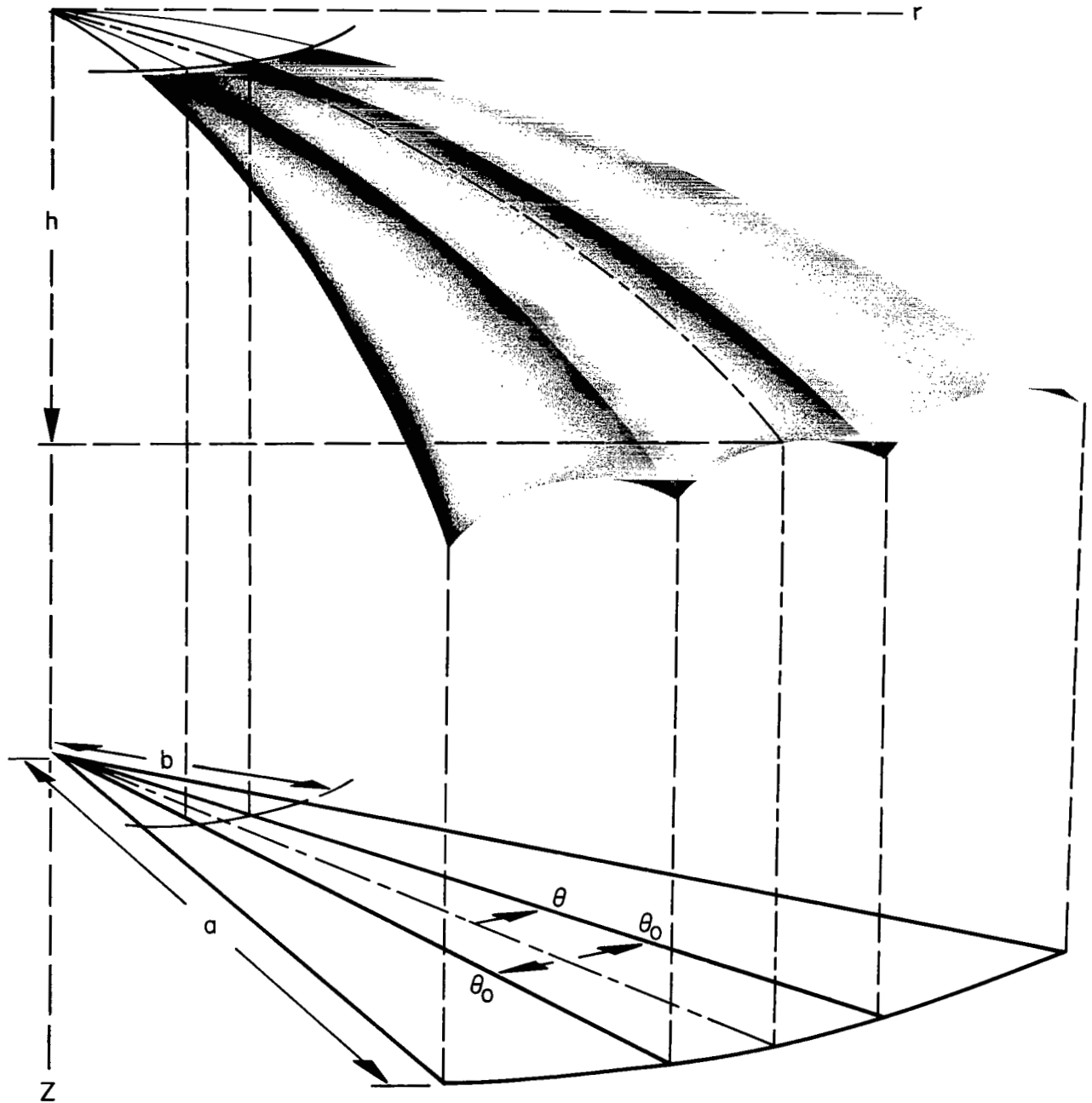


Figure 8.- Middle surface of the parachute type structure.

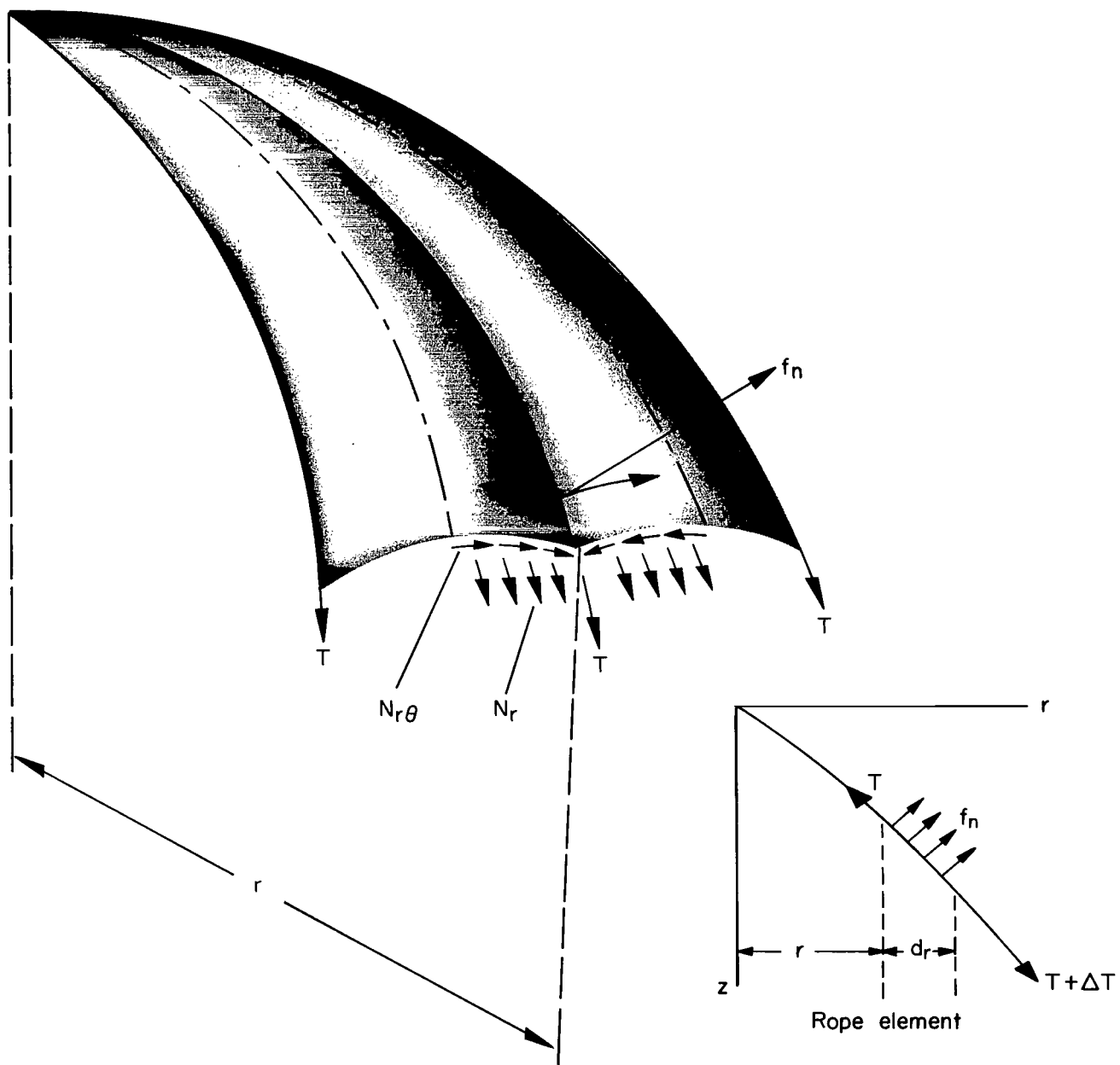


Figure 9.- Parachute type structure; condition for rope tension  $T$  at a radius  $r$ .

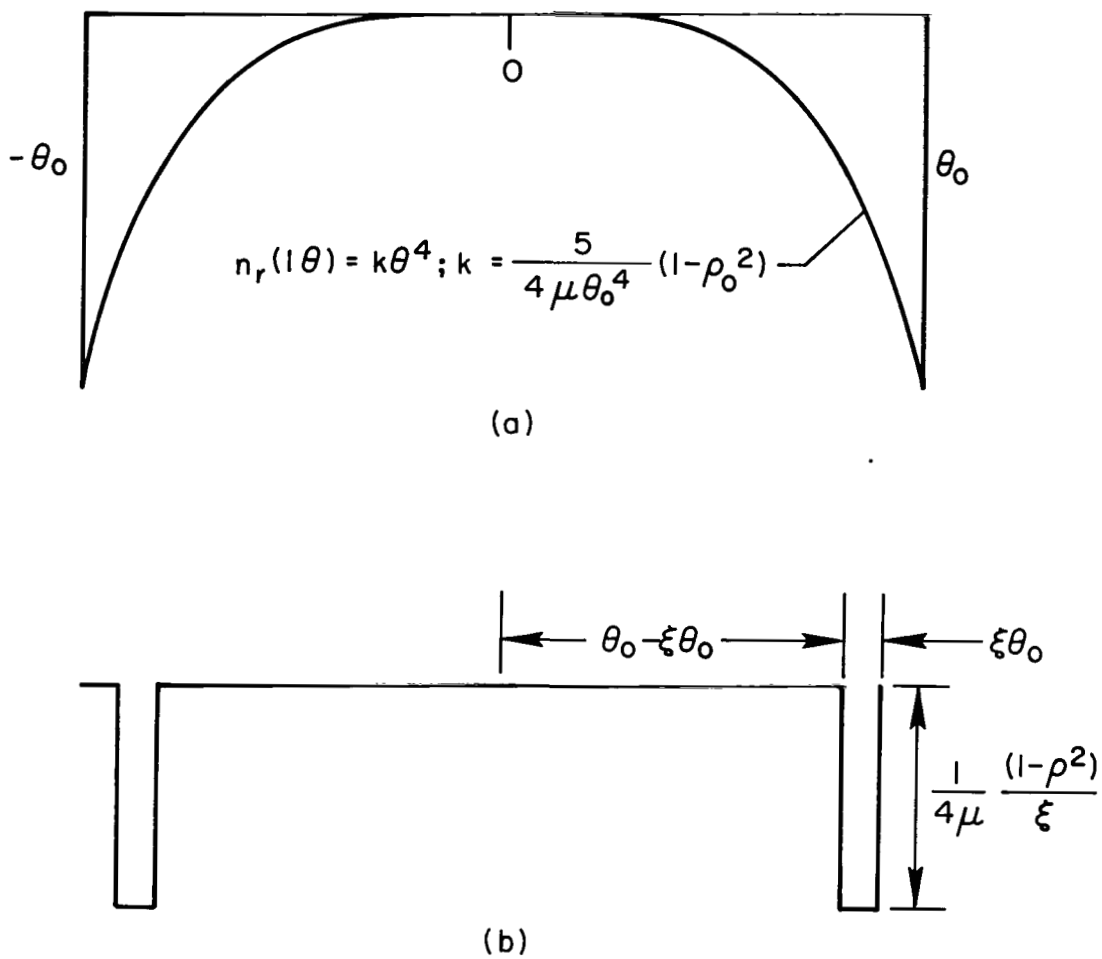


Figure 10.- Prescribable values of  $n_r(l, \theta)$  in a shell of revolution.



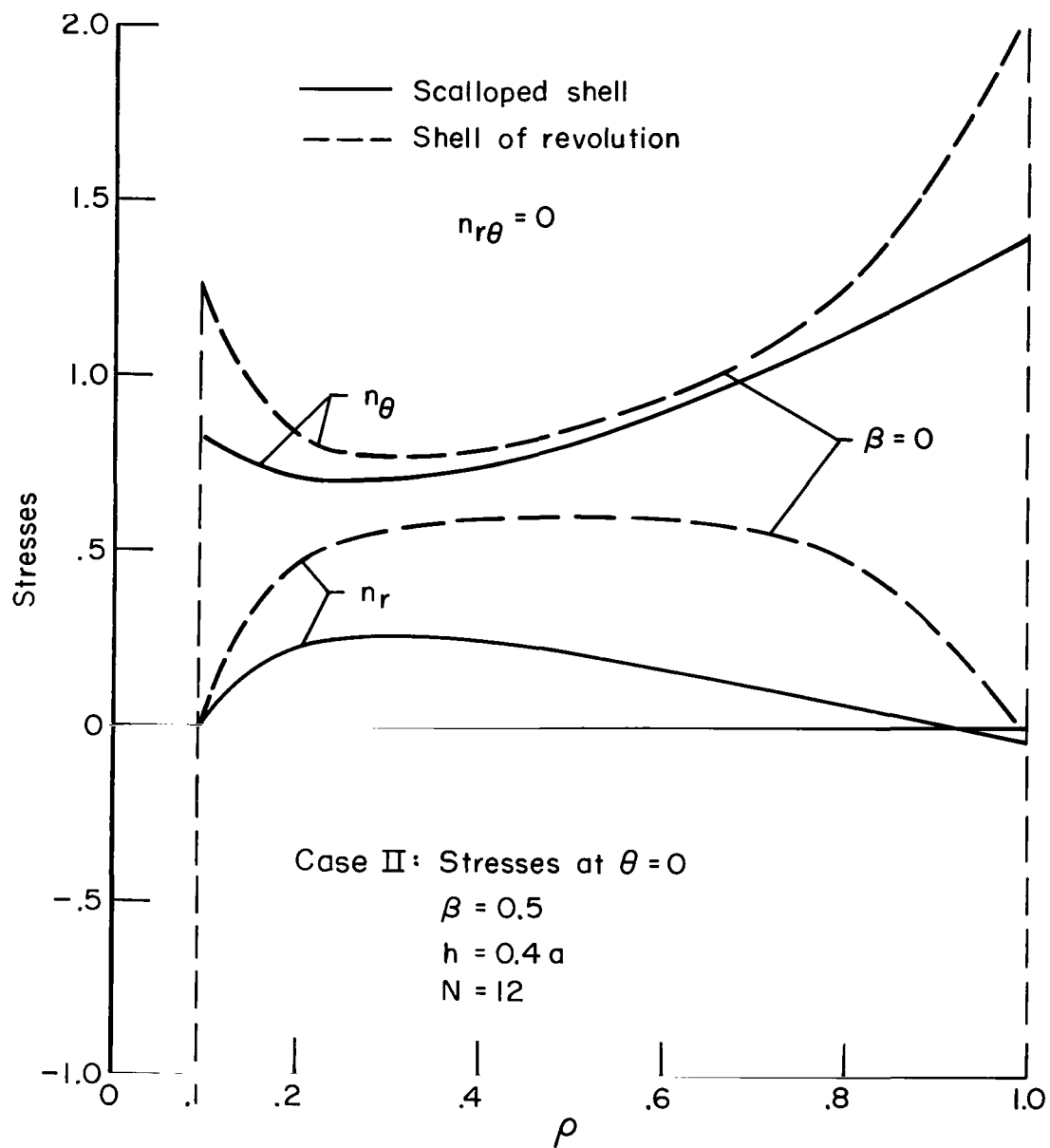


Figure 11.- Parachute type structure; membrane forces  $n_r$ ,  $n_\theta$  along the central meridian;  $\rho_0 = 0.1 \leq \rho \leq 1$ ;  $n_{r\theta} = 0$ .

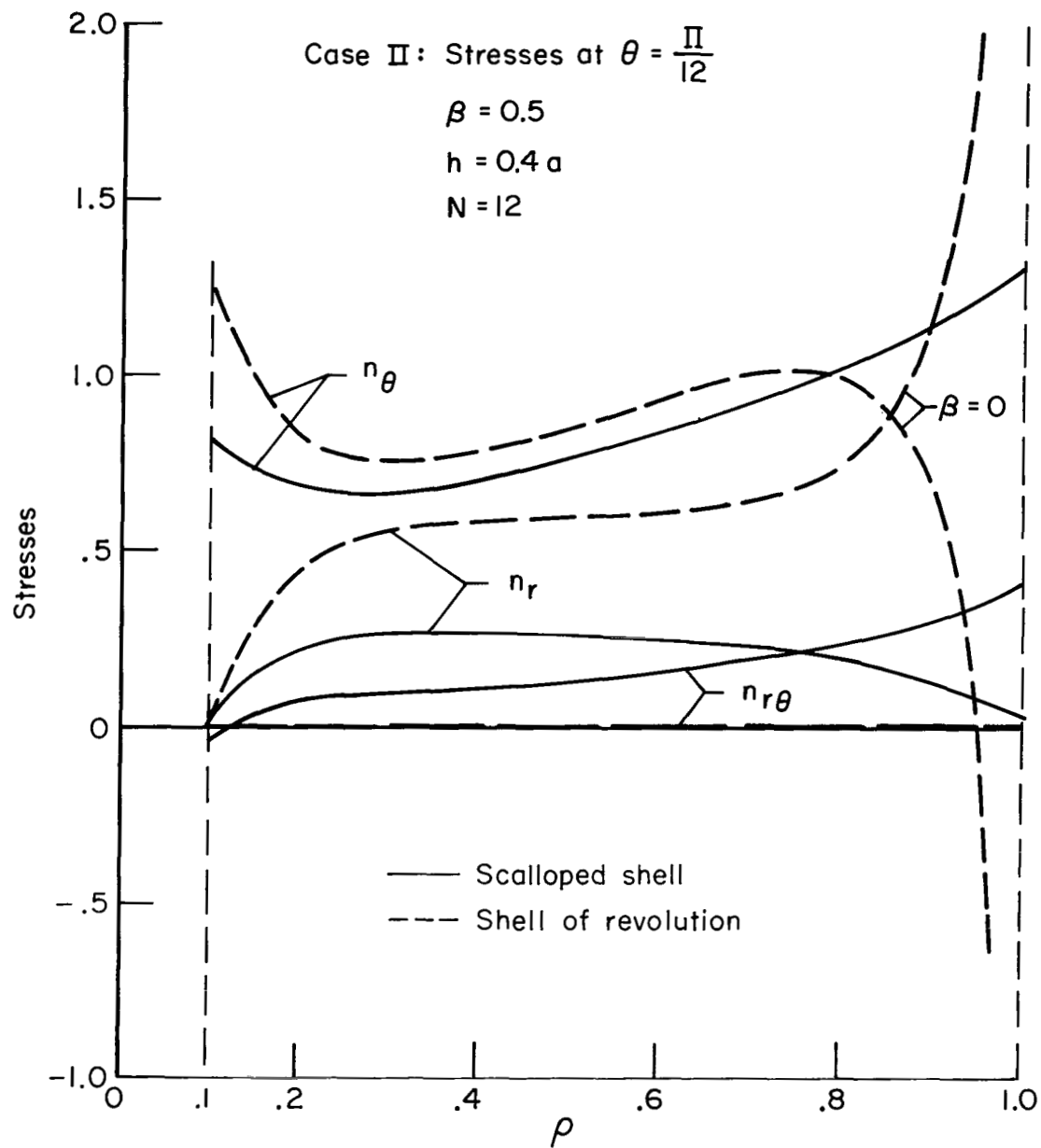


Figure 12.- Parachute type structure; membrane forces  $n_r$ ,  $n_\theta$ ,  $n_{r\theta}$  along the edge;  $x = x_0$ ;  $\rho_0 = 0.1 \leq \rho \leq 1$ .

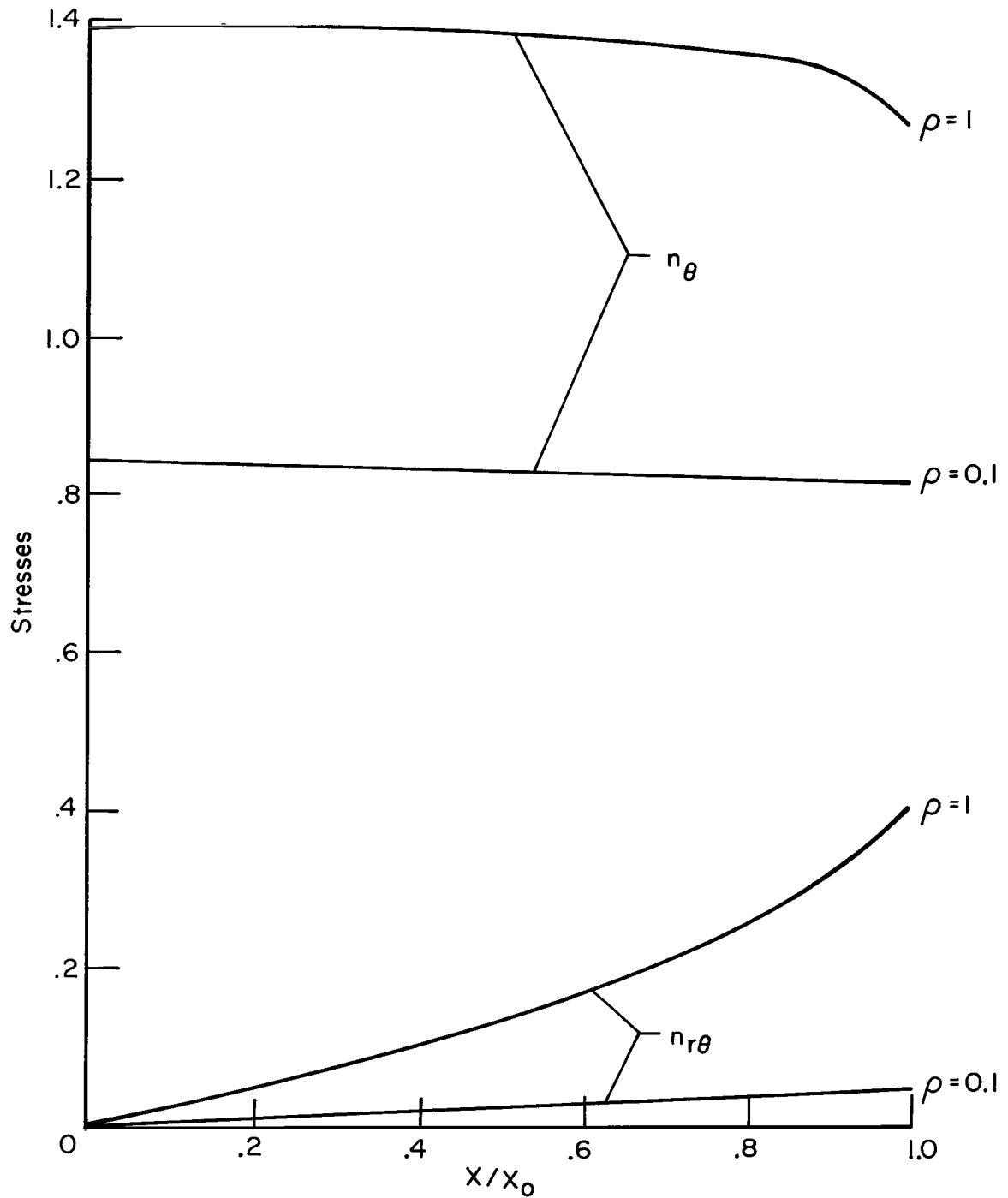


Figure 13.- Parachute type structure; membrane force  $n_\theta$  along the edge;  
 $\rho = \rho_0 = 0.1$  and  $\rho = 1$ ;  $0 \leq x \leq x_0$ .

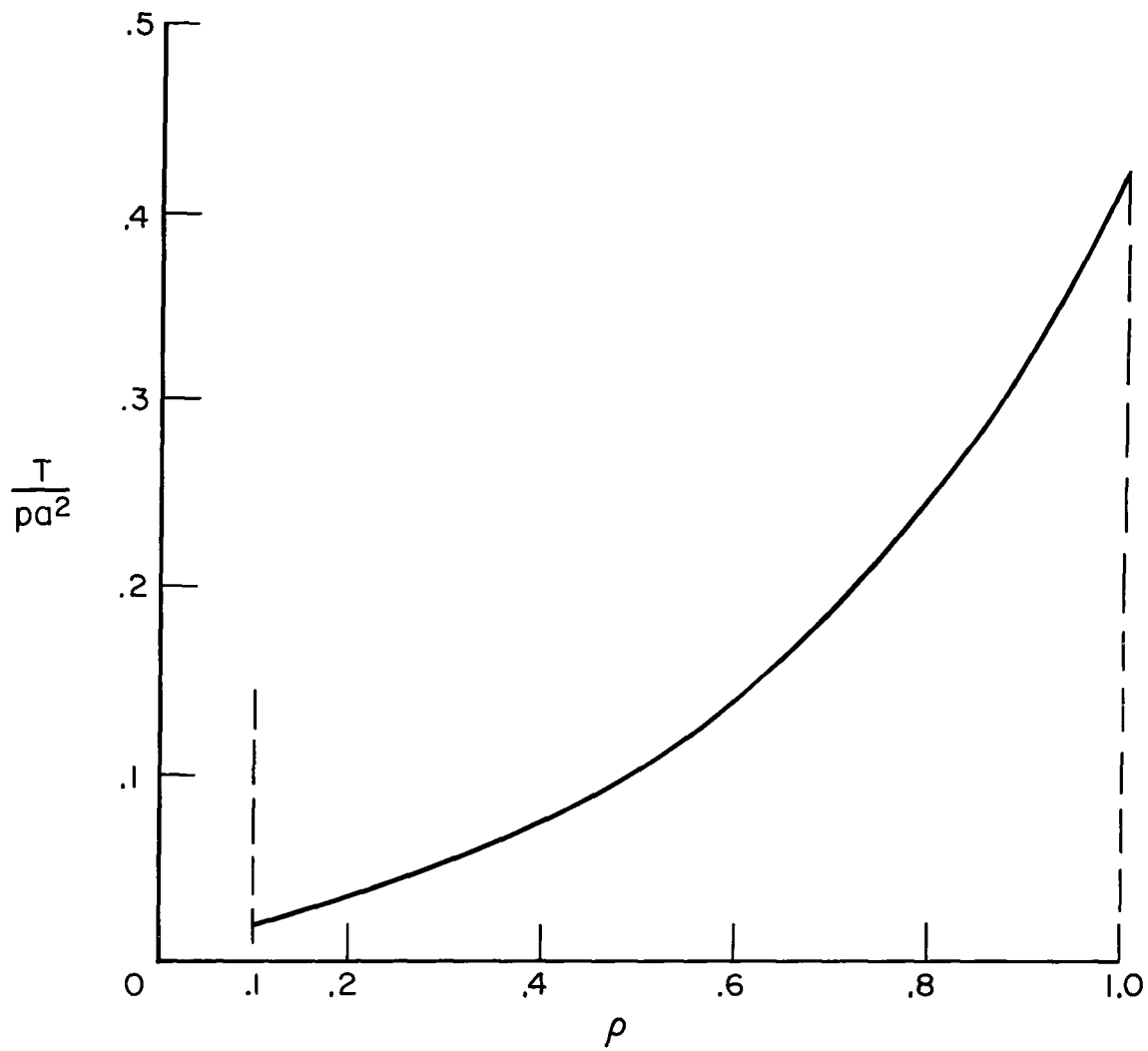


Figure 14.- Parachute type structure; rope tension  $T$ ;  $\rho_0 \leq \rho \leq 1$ .

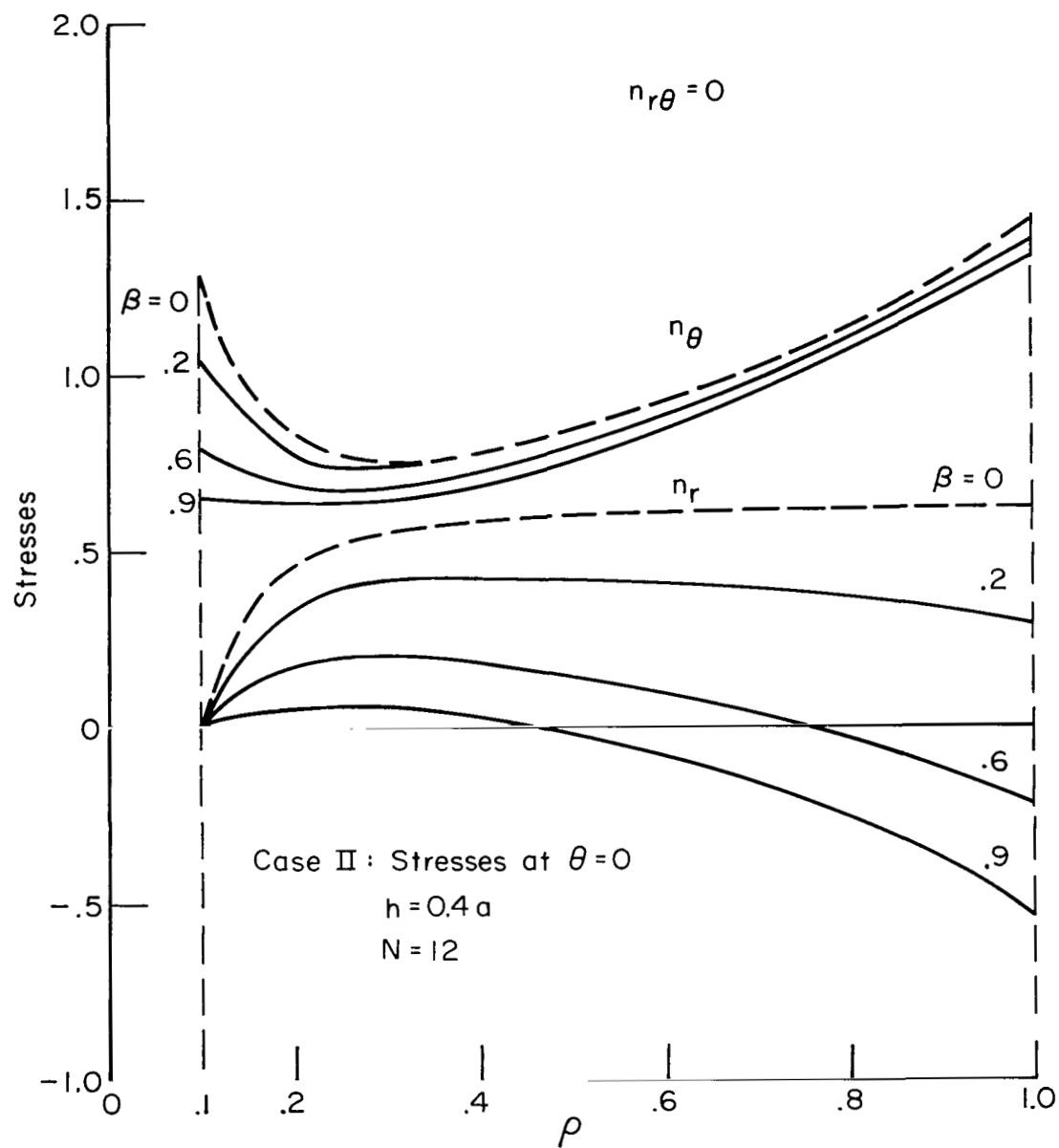


Figure 15.- Parachute type structure; membrane forces  $n_r$ ,  $n_\theta$  along the central meridian due to the solution  $\Psi_p$  for selected values of  $\beta$ ;  $\rho_0 \leq \rho \leq 1$ ;  $n_{r\theta} = 0$ .

030 011 57 51 305 68194 00903  
AIR FORCE WEAPONS LABORATORY/AFWL/  
KIRTLAND AIR FORCE BASE, NEW MEXICO 8711

ALL ALSO RECEIVED IN SALVA, CHIEF TECH  
LIBRARY 7-1117

POSTMASTER: If Undeliverable (Section 158  
Postal Manual) Do Not Return

*"The aeronautical and space activities of the United States shall be conducted so as to contribute . . . to the expansion of human knowledge of phenomena in the atmosphere and space. The Administration shall provide for the widest practicable and appropriate dissemination of information concerning its activities and the results thereof."*

— NATIONAL AERONAUTICS AND SPACE ACT OF 1958

## NASA SCIENTIFIC AND TECHNICAL PUBLICATIONS

**TECHNICAL REPORTS:** Scientific and technical information considered important, complete, and a lasting contribution to existing knowledge.

**TECHNICAL NOTES:** Information less broad in scope but nevertheless of importance as a contribution to existing knowledge.

**TECHNICAL MEMORANDUMS:** Information receiving limited distribution because of preliminary data, security classification, or other reasons.

**CONTRACTOR REPORTS:** Scientific and technical information generated under a NASA contract or grant and considered an important contribution to existing knowledge.

**TECHNICAL TRANSLATIONS:** Information published in a foreign language considered to merit NASA distribution in English.

**SPECIAL PUBLICATIONS:** Information derived from or of value to NASA activities. Publications include conference proceedings, monographs, data compilations, handbooks, sourcebooks, and special bibliographies.

**TECHNOLOGY UTILIZATION PUBLICATIONS:** Information on technology used by NASA that may be of particular interest in commercial and other non-aerospace applications. Publications include Tech Briefs, Technology Utilization Reports and Notes, and Technology Surveys.

*Details on the availability of these publications may be obtained from:*

SCIENTIFIC AND TECHNICAL INFORMATION DIVISION  
NATIONAL AERONAUTICS AND SPACE ADMINISTRATION  
Washington, D.C. 20546